

## Supplementary Materials for

### A small-molecule inhibitor of TRPC5 ion channels suppresses progressive kidney disease in animal models

Yiming Zhou,\* Philip Castonguay,\* Eriene-Heidi Sidhom, Abbe Clark, Moran Dvela-Levitt, Sookkyung Kim, Jonas Sieber, Nicolas Wieder, Ji Yong Jung, Svetlana Andreeva, Jana Reichardt, Frank Dubois, Sigrid C. Hoffmann, John M. Basgen, Mónica S. Montesinos, Astrid Weins, Ashley C. Johnson, Eric S. Lander, Michael R. Garrett, Corey R. Hopkins, Anna Greka<sup>†</sup>

\*These authors contributed equally to this work.

<sup>†</sup>Corresponding author. Email: agreka@bwh.harvard.edu

Published 8 December 2017, *Science* **358**, 1332 (2017)

DOI: 10.1126/science.aal4178

#### This PDF file includes:

Materials and Methods

Figs. S1 to S10

Tables S1 and S2

References

## **Materials and Methods**

### Animals

All animal studies were performed in accordance with Brigham and Women's Hospital, Harvard Medical School and University of Mississippi Medical Center (UMMC) institutional guidelines.

Littermates of wild-type (WT) and AT1R TgNeph-hAT1R/185 transgenic (AT1R Tg) Sprague-Dawley rats were housed under a controlled environment with a 12-hour light-dark cycle and access to food and water *ad libitum*, unless otherwise described. All animal experiments were performed in accordance to the guidelines established and approved by the Animal Care and Use Committee at Brigham and Women's Hospital, Harvard Medical School (Animal Protocol No. 01538). AT1R Tg rats were placed in the Onset cohort when measured proteinuria was > 5 mg/day (at approximately 12 weeks of age) on two separate 24-hour urine collections. AT1R Tg rats were placed in the Advanced cohort when measured proteinuria was > 25 mg/day (at approximately 18 weeks of age) on two separate 24-hour urine collections. These thresholds were determined after detailed histologic and phenotypic characterization of AT1R Tg rats compared to WT littermates (all combined, we studied n=91 WT rats and n = 122 AT1R Tg rats).

The Dahl salt-sensitive (S) inbred strain is maintained at University of Mississippi Medical Center (UMMC) and was originally obtained from University of Toledo-College of Medicine (SS/Jr). All animal experiments performed at UMMC were in accordance to the guidelines established and approved by our Institutional Animal Care and Use Committee. Animals used for this study were provided either low-salt diet [TD7034, 0.3% NaCl and/or high-salt diet [TD94217, 2.0% NaCl] from Harlan Teklad, Madison, WI. For onset study, at 4 weeks of age, groups of age-matched male S were weaned to the low-salt diet and divided into two groups: vehicle (n=8) and AC1903 groups (n=8). At 6 weeks of age, both groups were placed on the high-salt diet and concurrently treated with either vehicle or AC1903 for 1-week (Onset). For Advanced study, similarly at 4 weeks of age, groups of age-matched male S were weaned to the low-salt diet and divided into two groups: vehicle (n=9) and AC1903 groups (n=11). At 6 weeks of age, both groups were placed on the high-salt diet. At week 7, concurrent with high-salt diet, animals were treated with either vehicle or AC1903 for 1-week (Advanced). At the conclusion of each study, animals were initially anesthetized under 2-3% isoflurane/O<sub>2</sub> gas, a catheter attached to a fluid filled pressure transducer was placed in the aorta, isoflurane gas was reduced to 1.5%, and mean arterial pressure was measured for ~5 min period using PowerLab 4/30 system (ADI Instruments, Co) as done previously.

#### Chemical preparation and IP administration

All chemicals were purchased from Sigma-Aldrich unless otherwise described. ML204 and AC1903 were synthesized, purified and prepared by C. H. as powder in a single batch for each *in vivo* experiment to avoid variability. Immediately prior to injections, ML204 or AC1903 solution was placed on a heated shaker at 48°C and 800 RPM. Vehicle was prepared in the same fashion. Injection volume was determined by body weight (2mL vehicle/compound per kg body weight). Body weight was measured at the time of injection.

#### Urine collection and assay

For urine collections, rats were housed individually in a metabolic cage supplied with food and water. Urine was collected into a 50 mL falcon tube for 24 hours. Total urine volume was measured and then centrifuged at 3,200 rcf for 10 min at 4°C. Albumin quantification was done according to our previously published protocol (11), involving multiple dilutions of urine from each animal compared to Bovine Serum Albumin (BSA) standards. Coumassie Blue stained gels were quantified by densitometry using ImageJ software. As an additional control, the rat ELISA Albumin kit (Exocell) was used for albumin quantification according to the manufacturer's recommendations and yielded the same results.

#### Kidney preparation

Rats were anesthetized using pentobarbital sodium (50 mg/kg i.p.) and kidneys were perfused with ice-cold PBS. Kidneys were then perfused with 4% paraformaldehyde and stored in 4% glutaraldehyde solution. After embedding in resin, 1- $\mu$ m thick sections were cut and stained with toluidine blue. Light microscope images were obtained using a 100x oil lens with a final magnification of 1734x.

#### Acute glomeruli isolation and Ca<sup>2+</sup>-imaging

WT and AT1R Tg littermates were sacrificed and kidneys were quickly dissected and washed with ice-cold PBS. After isolation using the sieving technique as previously described (11), glomeruli were incubated with the Ca<sup>2+</sup> indicator Fura2-AM (1  $\mu$ M; Invitrogen) at 37 °C for 15 min. The extracellular solution for Ca<sup>2+</sup>-imaging contained (in mM) 140 NaCl, 5 KCl, 10 HEPES, 2 MgCl<sub>2</sub>, 2 CaCl<sub>2</sub>, 10 glucose with pH7.4 adjusted with NaOH. Glomerular Ca<sup>2+</sup>-imaging was performed using an inverted microscope

(Olympus IX70) with a high-speed CCD camera (Hamamatsu Photonics). Images were taken and analyzed using the Metafluor software (Molecular Devices). It should be noted that Fura-2 is most often taken up by podocytes at the periphery of the isolated glomerulus, but the specificity of recordings in podocytes is best confirmed by patch clamp electrophysiology, as described below.

#### Glomerular single-channel recordings

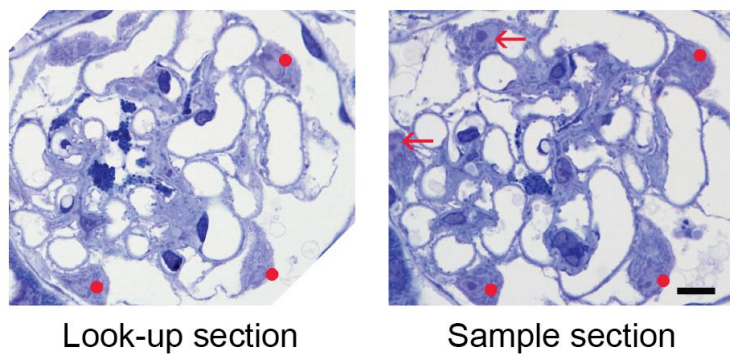
Acutely isolated glomeruli were prepared as described above. Single-channel recordings were carried out using an Axopatch 200B and Digidata 1550A (Molecular Devices). Bath and pipette solutions for glomerular single-channel recording contained (in mM) 135 CH<sub>3</sub>SO<sub>3</sub>Na, 5 CsCl, 2 CaCl<sub>2</sub>, 1 MgCl<sub>2</sub>, 10 HEPES, and 10 glucose with pH 7.4 adjusted with NaOH. Once in the inside-out configuration, the bath solution was replaced by intracellular solution, containing (in mM) 135 CH<sub>3</sub>SO<sub>3</sub>Cs, 10 CsCl, 3 MgATP, 0.2 EGTA, 0.13 CaCl<sub>2</sub>, and 10 HEPES with pH 7.4 adjusted with CsOH. Patch pipettes, with resistance of 4-8 MΩ, were prepared using a two step-protocol (P-97, Sutter Instrument). Pipettes were fire-polished before use. For inside-out configuration, a giga-seal (>10 GΩ) was established prior to membrane rupture. Data was acquired at 10 kHz sampling frequency, and filtered with low-pass filtering at 1 kHz. Holding membrane potential was at -60 mV. Single-channel analysis was carried out using Clampfit 10.4 software (Molecular Devices). NPo results were analyzed using the first 5 sec of Riluzole application and the last 5 sec of ML204 or AC1903 application.

#### Podocyte counting

For each kidney, serial 1-μm thick sections were cut from one or two resin blocks using an ultramicrotome fitted with a Histo Jumbo diamond knife (Diatome US, Hatfield, PA). After facing the block, the first technically good section was saved to a glass slide, labeled as slide 0, and stained with 0.5% toluidine blue. Subsequently, every 17th and 20th section were saved to a new slide, stained with toluidine blue and the slides labeled 20, 40, 60 etc. Thirty pairs of sections were saved from each kidney and used for podocyte counts. Images were obtained using a BX51 microscope with DP71 digital camera and DB Controller software (Olympus America, Inc., Cypress, CA). Using the 10x objective lens a map of all glomeruli present in section 0 was drawn. Glomeruli present on section 0 were necessarily incomplete and therefore could not be used for morphometric analysis. Next, the two sections on slide 20 were observed and compared to the map made of slide 0. Any new glomeruli appearing were sequentially numbered, drawn on the map, and imaged using the 100x lens. These and new glomeruli appearing

on subsequent slides were imaged using the subsequent pairs of sections until each glomerulus disappeared. The glomerular profiles on sections from the center of glomeruli were often larger than the field of view and 2-4 images were obtained and montaged to form a complete view of the glomerular profile. A stage micrometer was imaged and used to document the magnification of the images as 1734x. Image files were transferred to an Apple iMac Computer and viewed on a 24-inch monitor using Photoshop software (Adobe Systems, Inc., San Jose, CA). A Photoshop window magnification of 67% was used when making measurements.

Podocyte number per glomerulus was counted using the fractionator/disector method (16, 17). Podocyte nuclei were counted as a surrogate for the number of podocytes assuming one and only one nucleus per podocyte. Using the two images of a glomerulus from each pair of sections, the number of podocyte nuclei profiles seen in the first section (sample section) but not present in the second section (look-up section) was counted.



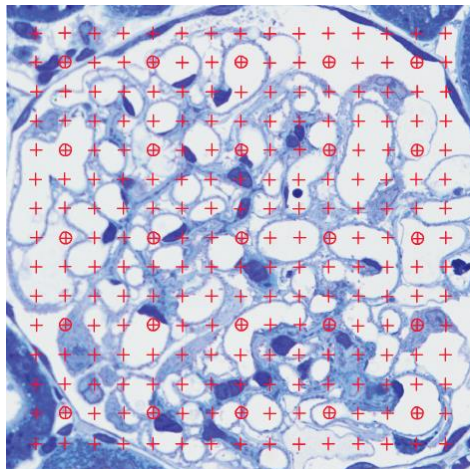
This was repeated for each pair of images from a glomerulus. The number of podocytes per glomerulus was calculated using the equation:

$$\text{Podocyte Number} = (20/3) \times \sum Q^-$$

where  $(20/3)$  is the reciprocal of the fraction of the glomerulus sample.  $\sum Q^-$  is the sum over all the section pairs from a glomerulus of nuclear profiles from podocytes seen in the sample sections but not in the look-up sections. Five glomeruli per kidney were analyzed and the average number of podocytes per glomerulus calculated.

### Pseudocyst volume per glomerulus

Pseudocyst volume per podocyte was calculated from Pseudocyst volume per glomerulus and podocyte number. Pseudocyst volume per glomerulus was measured on the images from the sample sections used to count podocyte number. First the volume density of pseudocysts per glomerulus [Vv (pseudocyst/glom)] was measured using point counting. A grid consisting of nine fine points (+) for each coarse point (+ with circle around it) was superimposed over each image (See below).



The number of fine points falling on the pseudocysts and the number of coarse points falling on glomerulus were counted and the volume density of pseudocysts per glomerulus calculated using the equation:

$$Vv(\text{pseudocyst/glom}) = \sum \text{FP} / (\sum \text{CP} \times 9)$$

where  $\sum \text{FP}$  is the sum of fine points falling on pseudocysts and  $\sum \text{CP}$  is the sum of coarse points falling on glomerulus. The number of coarse points falling on glomerulus is multiplied by 9 because there are nine times as many fine points as coarse points on the counting grid. Next the volumes of the glomeruli were measured using the Cavalieri Principle (17). The same images used to measure Vv(pseudocyst/glom) were used to measure glomerular volume. A new grid of points was superimposed over the images and the number of points falling on the glomerulus was counted. The volume of a glomerulus was calculated with the equation:

$$\text{Glomerular Volume} = \sum P \times 20 \times (50,000/1734)^2 \quad \mu\text{m}^3$$

where  $\Sigma P$  is the sum of points falling on a glomerulus over all the sample section images from the glomerulus, 20 is the distance in micrometers between the images measured, 50,000 is the distance in micrometers between grid points and 1734 is the magnification of the images. Squaring (50,000/1734) gives the area represented by each grid point at the level of the section in square micrometers. The Vv (pseudocyte/glm) is multiplied by the glomerular volume to get the total volume of pseudocytes in the glomerulus in cubic micrometers. The total volume of pseudocytes in the glomerulus divided by the number of podocytes in the glomerulus equals the volume of pseudocysts per podocyte in cubic micrometers. Five glomeruli per kidney were analyzed and the average pseudocyst volume per glomerulus for a rat calculated.

#### HEK293 cell culture and transfection

Transfection of Human embryonic kidney 293 (HEK293) cells was carried out using Plus reagent (Invitrogen) and Lipofectamine (Invitrogen) according to the standard protocols. For heterologous expression of TRP channels in HEK293 cells, 1  $\mu$ g of TRPC5-GFP, TRPC6-GFP or TRPC4 plasmids were used to transfet HEK293 cells in a 3.5 cm petri dish where cells were allowed to grow to 80% confluence. Electrophysiology was carried out after 16 h incubation.

#### HEK293 whole-cell recordings

Whole-cell patch clamp recording was performed 16 h after transfection. The bath solution contained (in mM): 140 NaCl, 5 KCl, 10 HEPES, 2 MgCl<sub>2</sub>, 2 CaCl<sub>2</sub>, 10 glucose with pH7.4 adjusted with NaOH. The intracellular solution contained (in mM): 140 KCl, 5 EGTA, 10 HEPES, 2 MgCl<sub>2</sub> with pH7.4 adjusted with KOH. The patch pipettes were made using a two-step-protocol (P-97, Sutter Instrument). The pipette resistance was maintained between 4 to 8 M $\Omega$ . Once the whole-cell configuration was achieved, cells were clamped at a holding potential of -60 mV, and given a 50 ms ramp stimulation from -100 mV to +100 mV in every 5 s. All currents were filtered at 2 KHz (Axopatch 200B amplifier, Axon Instruments, Union City, CA) and digitized at 10 KHz for whole-cell recordings using Axon pCLAMP 10.4. Data were then analyzed using Clampfit 10.4 (Molecular Devices).

#### Podocyte culture and viral transduction

Immortalized mouse podocytes were cultured as previously described (10, 11). Podocyte viral transduction was performed using lentivirus as previously described (10, 11).

Briefly, lentivirus production was carried out in HEK293 cells at 60% confluence, and viral particles were collected two days after transfection and purified by centrifugation at 1,000 rcf for 5 min. Purified lentivirus was frozen at -80°C until further use. Podocytes were transduced with lentivirus after 7 days of differentiation, and assays were performed 5 days after viral transduction.

#### ROS and cell viability assays

Mature podocytes were cultured as previously described. Cells were incubated with CellRox Deep Red reagent (ThermoFisher) for 30 min at 37°C. Then cells were washed with RPMI and treated with DMSO, 10 µM angiotensin II, 10 µM angiotensin II with 30 µM AC1903, or 10 µM angiotensin II with 30 µM N-acetyl- L-cysteine (NAC) for 3 h at 37°C. Cells were washed with PBS twice and fluorescence images were observed using Olympus IX71 microscopy. Fluorescence intensities were then analyzed using ImageJ software.

For experiments in Figure 2E-F, pCDNA3.1 AT1AR- Δ324 (rat AT1R NM\_030985.4) containing HA tag (Plasmid #45635, Addgene) underwent site directed mutagenesis (Agilent) to generate the N111S substitution as a constitutive activated form of AT1R (caAT1R). For Fig. 2E, differentiated podocytes were transduced with the AT1A-N111S/Δ324 construct in six-well plates. Six days after viral transduction, cells were treated with either vehicle, 30 µM ML204, 30 µM AC1903 or 50 µM NSC23677 for 36 h. Intracellular production of ROS was measured using a cell-permeable fluorescent dye, 5-(and-6)-chloromethyl-2',7'-dichlorodihydrofluorescein diacetate, acetyl ester (CM-H<sub>2</sub>DCFDA, Molecular Probes). Cells were incubated with 5µM CM-H<sub>2</sub>DCFDA at 37°C for 45 min in Hanks' balanced salt solution (HBSS). Cells were then collected, resuspended in HBSS, stained with propidium iodide and the fluorescence intensity was assessed by flow cytometry using MACSQuant Analyzer (Miltenyi Biotec, Bergisch Gladbach, Germany). Living cells, which were PI negative, were selected by FACS gating and the fluorescence of CM-H<sub>2</sub>DCFDA was recorded on the FL-1 channel (525 nm). For Fig. 2F, differentiated podocytes were transduced with the AT1A-N111S/Δ324 construct in 96 well plates. Six days after transduction, the cells were treated with either vehicle, 30 µM ML204, 30 µM AC1903 or 50 µM NSC23677 for 36 h. Cell viability assays were performed using Cell Titer-Glo Luminescent Cell Viability Assay kits (Promega) and a luminometer (Veritas Microplate Luminometer) according to the manufacturer's protocol.

### In-Vivo Pharmacokinetic Studies

*In-vivo* pharmacokinetic (PK) experiments were performed at Vanderbilt University. All PK studies were conducted in accordance with the National Institute of Health regulations of animal care covered in Principles of Laboratory Animal Care (National Institutes of Health publication 85-23, revised 1985) and were approved by the Institutional Animal Care and Use Committee at Vanderbilt University. Discrete PK experiments in male Sprague-Dawley (SD) rats ( $n=2$ ) were carried out at a dose of 25 mg/kg, intraperitoneally (i.p.), in either PBS (ML204) or 10% EtOH, 40% PEG 400, 50% saline or 5% DMSO, 10% Tween80, 85% PBS (AC1903). Each dose was administered i.p. to dual-cannulated (carotid artery and jugular vein) adult male SD rats, each weighing between 250 and 350 g (Harlan, Indianapolis, IN). Whole blood collections via the carotid artery were performed at 0.033, 0.117, 0.25, 0.5, 1, 2, 4, 7, and 24 hours post-dose and plasma samples were prepared for analysis. *In vivo* samples were analyzed via electrospray ionization (ESI) on an AB Sciex API-4000 (Foster City, CA) triple-quadrupole instrument that was coupled with Shimadzu LC-10AD pumps (Columbia, MD) and a Leap Technologies CTC PAL auto-sampler (Carrboro, NC). Analytes were separated by gradient elution using a Fortis C18 3.0 x 50 mm, 3  $\mu$ m column (Fortis Technologies Ltd, Cheshire, UK) thermostated at 40 °C. HPLC mobile phase A was 0.1% formic acid in water (pH unadjusted), mobile phase B was 0.1% formic acid in acetonitrile (pH unadjusted). The source temperature was set at 500 °C and mass spectral analyses were performed using multiple reaction monitoring (MRM), with transitions specific for each compound utilizing a Turbo-Ionspray® source in positive ionization mode (5.0 kV spray voltage). The calibration curves were constructed, and linear response was obtained by spiking known amounts of test compound in blank brain homogenate or plasma. All data were analyzed using AB Sciex Analyst software v1.5.1. The final PK parameters were calculated by noncompartmental analysis using Phoenix (version 6.2) (Pharsight Inc., Mountain View, CA).

### Glomerular RNA isolation

Glomerular RNA isolation was performed using the Trizol reagent (Ambion, Life Technologies) according to the manufacturer's protocol. Briefly, acutely isolated glomeruli were homogenized in 1 mL Trizol reagent on ice. After adding 200 $\mu$ L chloroform, the solution was vigorously mixed and centrifuged 12,000 rcf at 4 °C for 15 min. The aqueous layer was carefully transferred into a new tube. Glomerular RNA was precipitated after adding 500  $\mu$ L isopropanol by centrifugation 12,000 rcf at 4 °C for 10 min and then washed with 1 mL 70% ethanol. After centrifugation 12,000 rcf at 4 °C for

5 min, the glomerular RNA pellet was allowed to air dry completely and was then dissolved in 15  $\mu$ L nuclease-free water.

### Gene Transcriptional Profiling

#### *cDNA Library Construction*

RNA was quantified using the Quant-iT™ RiboGreen® RNA Assay Kit (Thermo Scientific #R11490) and normalized to 5ng/ $\mu$ L. An automated variant of the Illumina TruSeq™ Stranded mRNA Sample Preparation Kit was used for library preparation from a 200 ng aliquot of RNA. This method preserves strand orientation of the RNA transcript and uses oligo dT beads to select mRNA from the total RNA sample. Following cDNA synthesis and enrichment, cDNA libraries were quantified with qPCR using KAPA Library Quantification Kit for Illumina Sequencing Platforms and then pooled equimolarly.

#### *Illumina Sequencing*

Pooled libraries were normalized to 2 nM and denatured using 0.1 N NaOH prior to sequencing. Flowcell cluster amplification and sequencing were performed according to the manufacturer's protocols using either the HiSeq 2000 or HiSeq 2500. Each run was a 101 bp paired-end with an eight-base index barcode read. Data was analyzed using the Broad Institute Picard Pipeline, which includes de-multiplexing and data aggregation. Original fastq files are available in GEO (GSE103020).

#### *RNA-Seq and Differential Expression Analysis*

Reads were aligned to the Rnor\_5.0 rat genome using STAR aligner. RSEM v1.3.0 was used to estimate gene expression. FastQC was used to evaluate the quality of raw reads. Low count features were filtered using NOISeq with an expression threshold of > 1 count per million per condition (35). Differential expression of individual genes was carried out using DESeq2 (36). Only genes with adjusted p-values < 0.05 were considered to be differentially expressed. Gene Ontology analysis was performed using GOrilla. The specific gene ontologies cited in Figure S8: (C) GO:0016491, GO:0015075, GO:0022857, GO:0016614, GO:0008324, GO:0051287, GO:0016829, GO:0016651, GO:0050661; (D) GO:0031589, GO:0007166, GO:0007155, GO:0007229.

#### **Statistical analysis**

All statistical analyses were carried out using Graphpad Prism 6 software. Results are presented as Mean  $\pm$  SEM unless otherwise indicated. The comparisons were carried out

using the Student's t-test or ANOVA followed by *post-hoc* comparison using the Bonferroni test.  $P < 0.05$  was considered statistically significant.

## **Supplementary Figures**

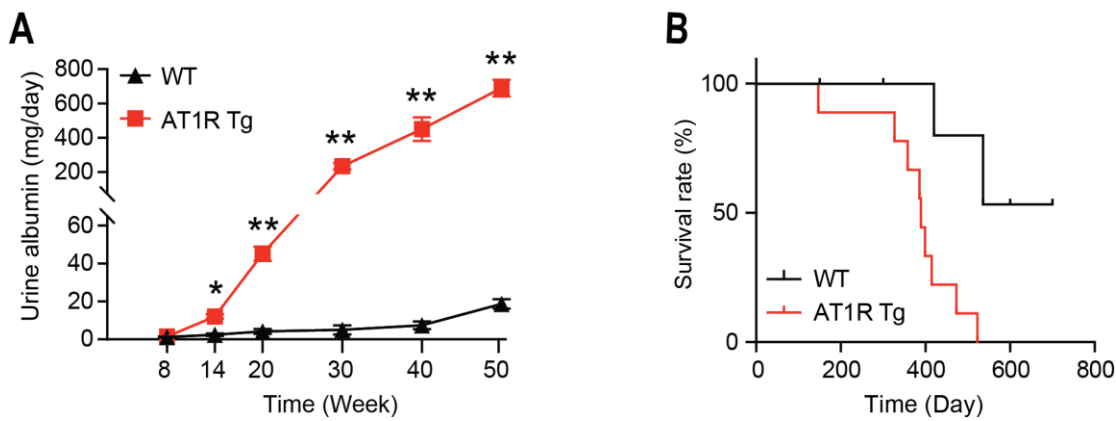


**Fig. S1. Podocyte-specific AT1R Tg rats develop progressive, severe proteinuria.**

(A) Proteinuria in AT1R Tg rats over the course of 50 weeks, with onset of disease at ~8 weeks and severe escalation in proteinuria beyond 14 weeks. WT n = 91, AT1R Tg n = 122. Mean ± SEM, \*p < 0.05, \*\*p < 0.01.

(B) Survival curves for AT1R Tg rats compared to WT controls. WT n = 10, AT1R Tg n = 9.

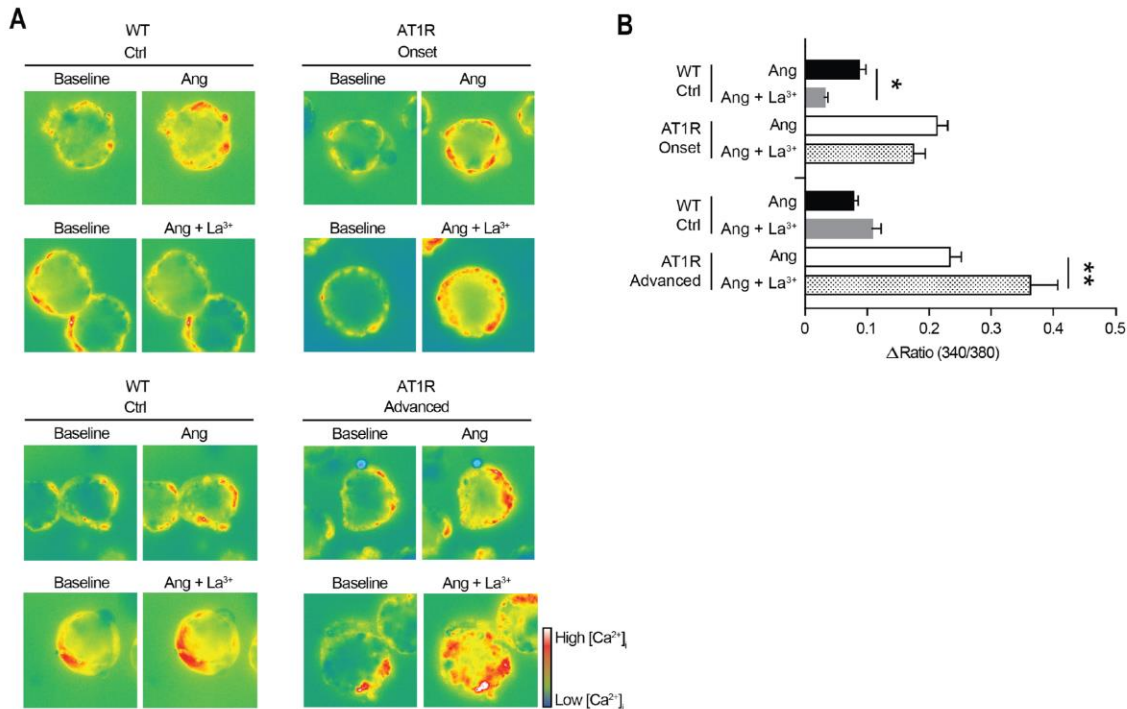


**Fig. S2. Increased TRPC5 channel activity correlates with FSGS disease progression.**

(A) La<sup>3+</sup> suppresses the AngII-mediated podocyte Ca<sup>2+</sup> influx in isolated glomeruli from WT rats. Ang-II mediated Ca<sup>2+</sup> influx is resistant to block by La<sup>3+</sup> during disease onset (Onset) in isolated glomeruli from AT1R Tg rats, thus unmasking the contribution of La<sup>3+</sup>-potentiated TRPC5 channels. Significantly increased podocyte Ca<sup>2+</sup> was noted in rats with established disease (Advanced), reinforcing the conclusion that TRPC5 channel activity drives the AngII-mediated Ca<sup>2+</sup> influx during disease progression.

(B) Ratiometric Ca<sup>2+</sup> imaging quantification in isolated rat glomeruli. WT Ang n = 123 and 89, WT Ang + La<sup>3+</sup> n = 116 and 84, AT1R Tg Ang n = 69 and 102, AT1R Tg Ang + La<sup>3+</sup> n = 87 and 65 for Onset and Advanced groups, respectively, each from > 6 independent replicates. Mean ± SEM, \*p < 0.05, \*\*p < 0.01.

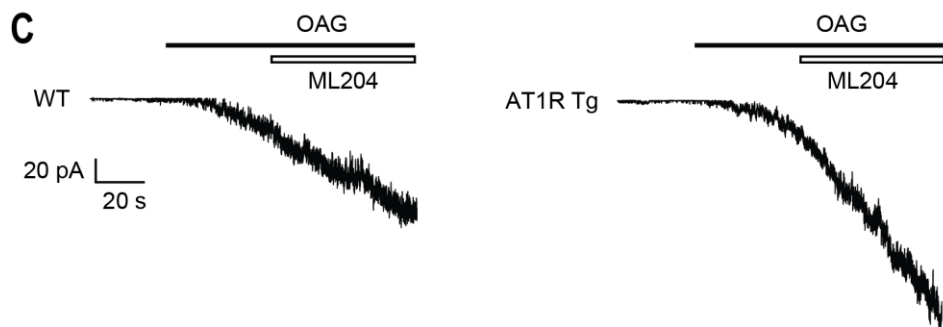
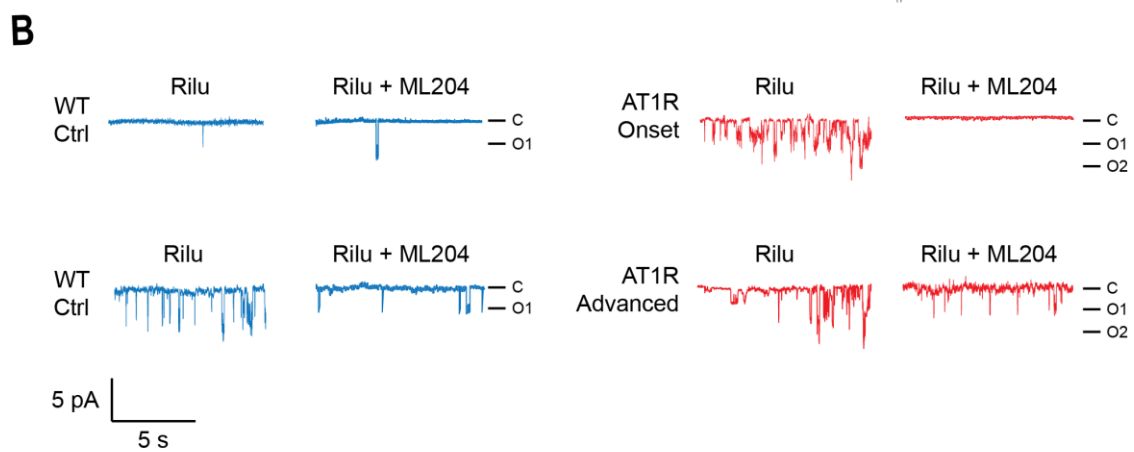
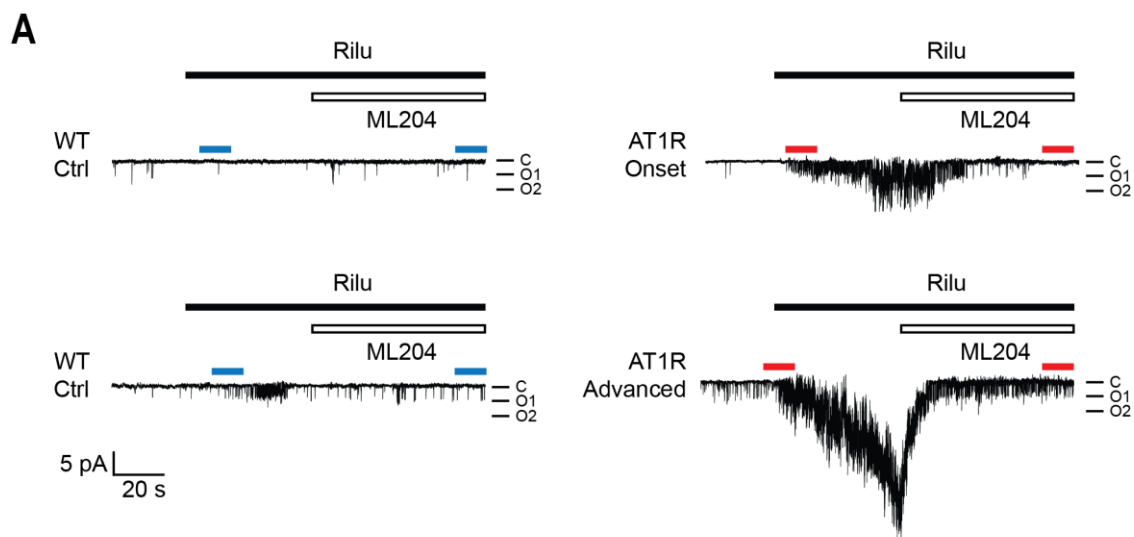


**Fig. S3. ML204 blocks TRPC5 but not TRPC6 single-channel activity.**

(A) ML204 (1  $\mu$ M) blocks TRPC5 channel activity induced by Riluzole (Rilu, 3  $\mu$ M) in inside-out recordings from rat glomeruli isolated at disease onset (Onset), as compared to barely detectable current in age matched WT rat glomeruli (Onset). ML204 blocks a significantly greater Rilu-activated conductance in glomeruli isolated from rats with established disease (Advanced), compared to minimal TRPC5 activity in age matched WT glomeruli (Advanced). C, close state, O<sub>1</sub>, open channel level 1, O<sub>2</sub>, open channel level 2.  $V_m = -60$  mV.

(B) Magnified single-channel recording traces before and after ML204. Colored bars in A correspond to colored traces (blue, red).

(C) ML204 does not block OAG-induced conductances in recordings from age matched AT1R Tg rats after established, advanced disease compared to age matched WT controls.

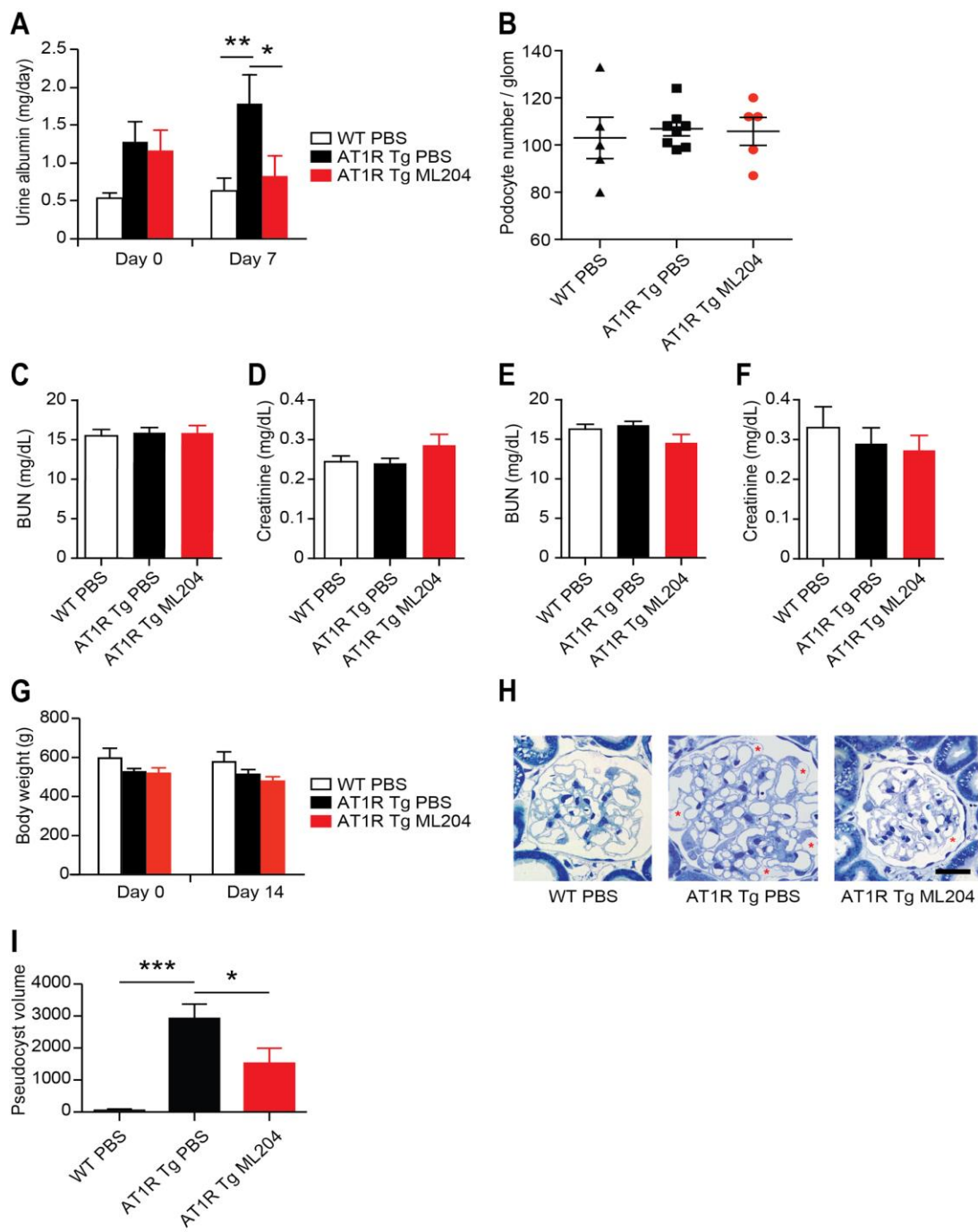


**Fig. S4. ML204 blocks proteinuria to complete remission at disease onset, and prevents pseudocyst formation in animals with advanced disease.**

(A) ML204 blocks proteinuria at disease onset in AT1R Tg rats. Treated animals are indistinguishable from WT controls after 7 days of treatment (25 mg/kg i.p. twice a day). WT PBS n = 5, AT1R Tg PBS n = 8, AT1R Tg ML204 n = 5. Mean ± SEM, \*p < 0.05, \*\*p < 0.01.

(B) No loss of podocytes before or after ML204 treatment during early stages of disease (Onset). WT PBS n = 5, AT1R Tg PBS n = 8, AT1R Tg ML204 n = 5. Mean ± SEM.

(C, D) Unchanged BUN and creatinine in AT1R Tg rats treated with ML204 at disease onset. WT PBS n = 3, AT1R Tg PBS n = 5, AT1R Tg ML204 n = 3. Mean ± SEM.

(E, F) Unchanged BUN and creatinine in AT1R Tg rats treated with ML204 during advanced, established disease. WT PBS n = 4, AT1R Tg PBS n = 8, AT1R Tg ML204 n = 5. Mean ± SEM.

(G) ML204 does not affect rat body weight. WT PBS n = 7, AT1R Tg PBS n = 13, AT1R Tg ML204 n = 8. Mean ± SEM.

(H) Toluidine blue semithin sections of rat kidneys. Red asterisks indicate podocyte pseudocysts. This is observed in AT1R Tg rat sections, but not in AT1R Tg rats treated with ML204, similar to WT controls. Size bar, 50 µM.

(I) Reduction of pseudocyst volume in AT1R Tg ML204 rats compared to AT1R Tg PBS rats. WT PBS n = 7, AT1R Tg PBS n = 9, AT1R Tg ML204 n = 8. Mean ± SEM, \*p < 0.05, \*\*\*p < 0.001.

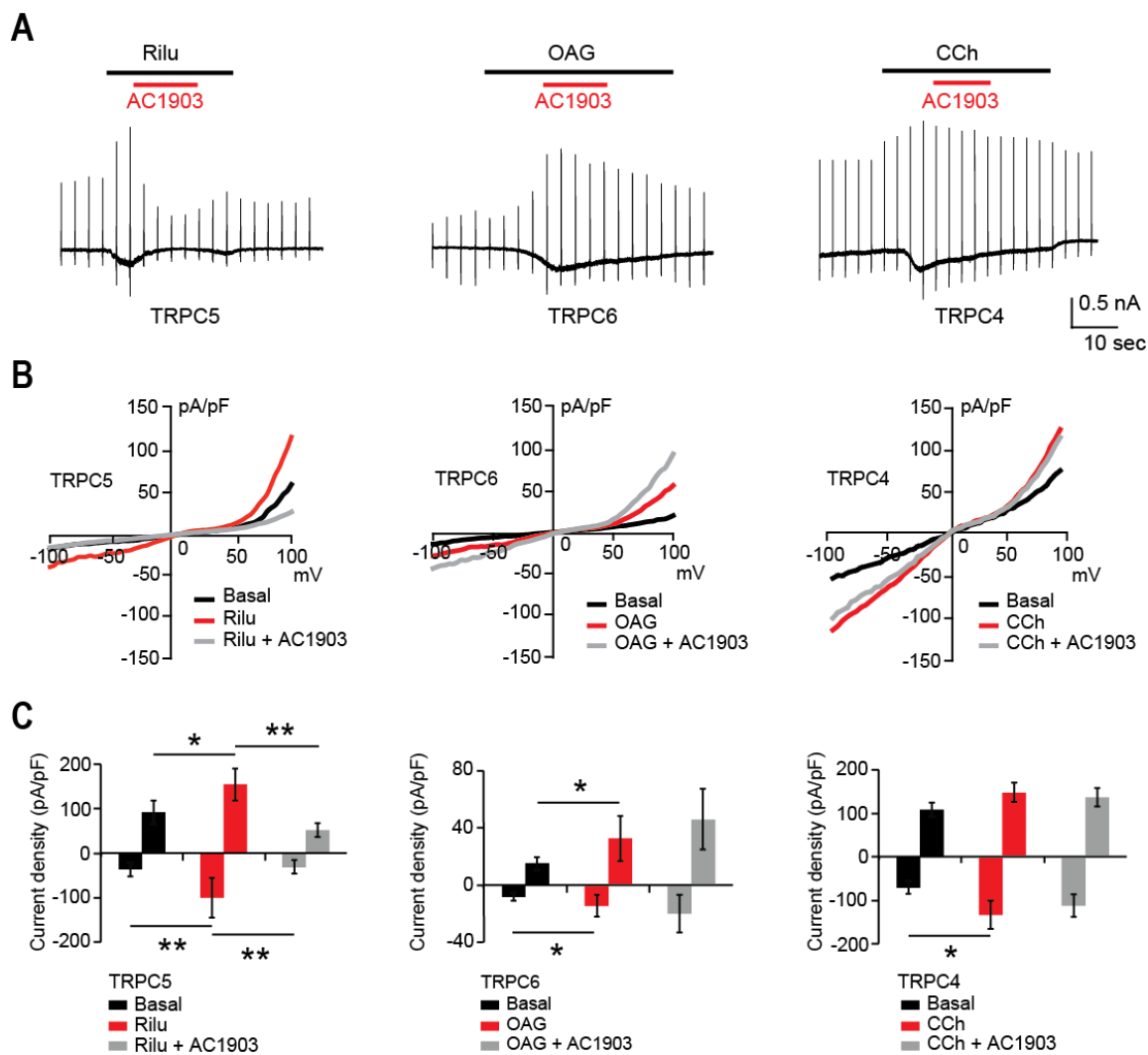


**Fig. S5. AC1903 is a specific inhibitor of TRPC5 ion channels.**

(A) Representative whole-cell current recordings of AC1903 effects on TRPC5, TRPC6 and TRPC4 channels. AC1903 (30  $\mu$ M) blocks Rilu-activated TRPC5 whole cell conductance in HEK cells expressing TRPC5. No AC1903 effect on OAG-activated (30  $\mu$ M) TRPC6 channel activity or CCh-activated (100  $\mu$ M) TRPC4 channel activity.

**(B)** Representative current-voltage (I-V) relationships show that AC1903 specifically inhibits TRPC5 channel activity versus TRPC6 and TRPC4 channel activity. Current density in pA/pF.

**(C)** Quantification of current densities (pA/pF) from whole cell recordings. AC1903 specifically inhibits TRPC5-mediated inward and outward current, but does not inhibit TRPC6 or TRPC4 currents. TRPC5 n = 6, TRPC6 n = 6, TRPC4 n = 5. Mean  $\pm$  SEM, \*p < 0.05, \*\*p < 0.01.

Analyte	AC1903	Analyte	ML204
Study	IP PK	Study	IP PK
Animals	Rat SD, male (N=2)	Animals	Rat SD, male (N=2)
Vehicle	IP: 10% EtOH, 40% PEG400, 50% saline	Vehicle	IP: sterile PBS
Dose	IP 25 mg/kg	Dose	IP 20 mg/kg
Matrix	EDTA plasma	Matrix	EDTA plasma
MW	303.4	MW	226.3
LLOQ	0.5-10 ng/mL depending on analyte	LLOQ	0.5 ng/mL
Salt MW 339.8			
Salt MW 262.8			

AC1903				ML204			
Dose (mg/kg)	Time (hr)	Concentration (ng/mL)		Dose (mg/kg)	Time (hr)	Concentration (ng/mL)	
		1	2			1	2
25	0.25	637	1180	909	20	0.25	1490
	0.5	349	557	453		0.5	825
	1	196	293	245		1	542
	2	149	138	144		2	320
	4	35.2	37.6	36.4		4	129
	7	12.4	14.9	13.7		7	55.1
	24	2.91	4.54	3.73		24	BLQ
PK Parameter		1	2	Mean	PK Parameter		1
Cmax	ng/mL	637	2420	1529	Cmax	ng/mL	1490
Tmax	hr	0.250	0.117	0.184	Tmax	hr	0.25
AUC (PO)	hr*ng/mL	950	1566	1258	AUC (PO)	hr*ng/mL	2133
							3569
							2851

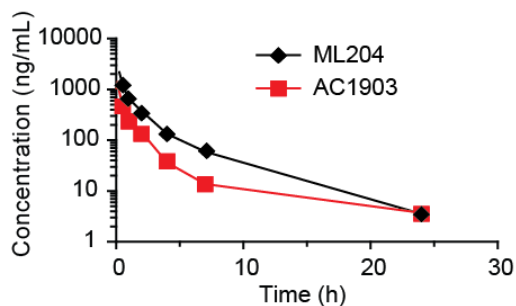


**Fig. S6. Pharmacokinetic (PK) studies in Sprague-Dawley rats comparing ML204 and AC1903.**

Minimum concentration, maximum concentration ( $C_{\max}$ ) and area under the curve (AUC) measurements are shown after single injection of each drug. Please see Methods for more details. These PK data were utilized to select the dosing regimen and administration protocol for AC1903. The dose of 50 mg/kg of AC1903 was chosen based on the  $IC_{50}$  values of this compound compared to ML204, and given PK exposure at 25 mg/kg.

ML204 had ~2-time higher AUC exposure (and C<sub>max</sub>) and thus the dose of AC1903 was increased to replicate the exposure levels of ML204.

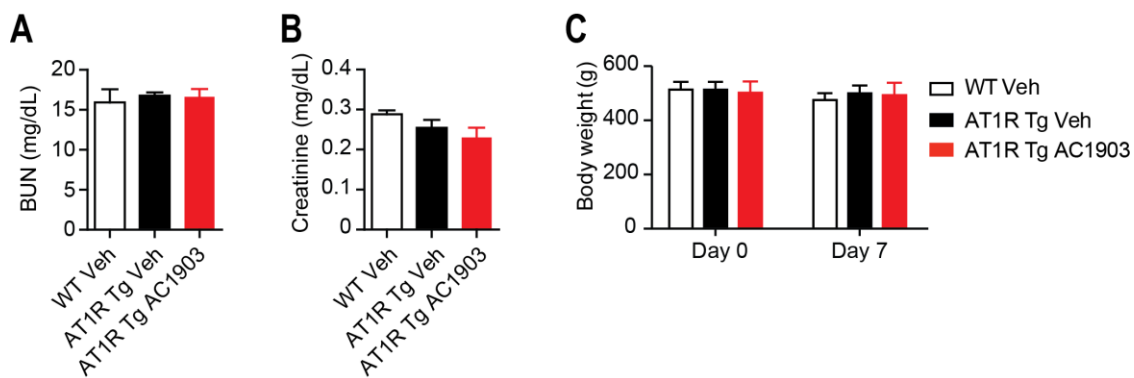


**Fig. S7. Chronic administration of AC1903 does not affect BUN, creatinine or body weight in AT1R Tg rats.**

(A) Unchanged BUN in AT1R Tg rats with advanced, established disease treated with AC1903. WT Veh n = 4, AT1R Tg Veh n = 7, AT1R Tg AC1903 n = 6. Mean ± SEM.

(B) Unchanged creatinine during chronic administration of AC1903. WT PBS n = 4, AT1R Tg PBS n = 7, AT1R Tg AC1903 n = 6. Mean ± SEM.

(C) Unchanged body weights during chronic administration of AC1903 for 7 days. WT Veh n = 4, AT1R Tg Veh n = 7, AT1R Tg AC1903 n = 6. Mean ± SEM.

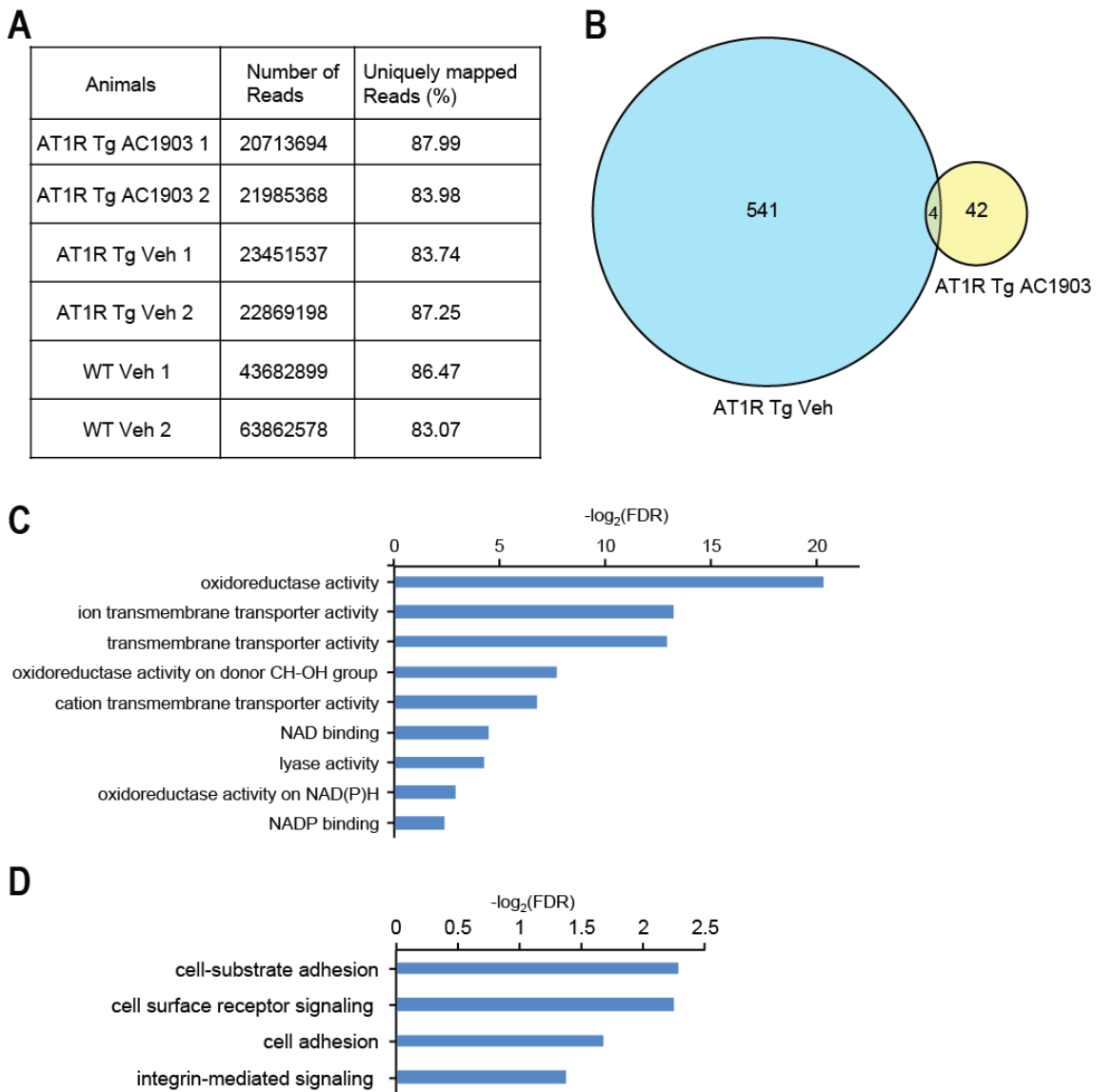


**Fig. S8. RNASeq analysis of AT1R Tg AC1903 rats compared to AT1R Tg PBS and WT controls in the Advanced cohort.**

(A) Overview of obtained and uniquely mapped reads.

- (B)** Venn diagram analysis of differentially expressed genes (adjusted p-value < 0.05) in AT1R Tg rats (compared to WT) and in AT1R Tg rats treated with AC1903 (compared with AT1R Tg rats treated with vehicle).
- (C)** Gene Ontology enrichment analysis of differentially expressed genes in AT1R Tg animals (compared to WT).
- (D)** Gene Ontology enrichment analysis of genes differentially expressed in AC1903-treated Tg animals (compared to vehicle treated AT1R Tg rats).

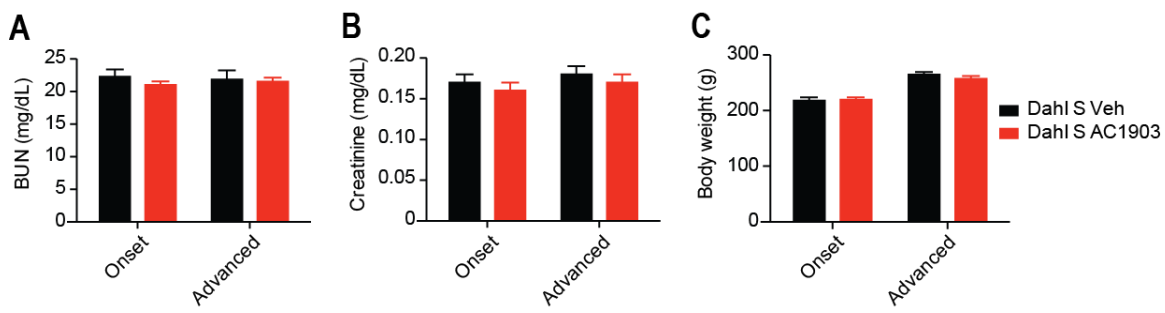


**Fig. S9. Chronic administration of AC1903 does not affect BUN, creatinine or body weight in Dahl S rats.**

(A) Unchanged BUN in Dahl S rats treated with AC1903 in two independent studies, Onset and Advanced. Dahl S Veh n = 8 and 9, Dahl S AC1903 n = 8 and 14 for Onset and Advanced, respectively. Mean  $\pm$  SEM.

(B) Unchanged creatinine in Dahl S rats treated with AC1903 in two independent studies. Dahl S Veh n = 8 and 9, Dahl S AC1903 n = 8 and 14 for Onset and Advanced, respectively. Mean  $\pm$  SEM.

(C) Unchanged body weights during chronic administration of AC1903 in Dahl S rats in two independent studies. Dahl S Veh n = 8 and 9, Dahl S AC1903 n = 8 and 14 for Onset and Advanced, respectively. Mean  $\pm$  SEM.

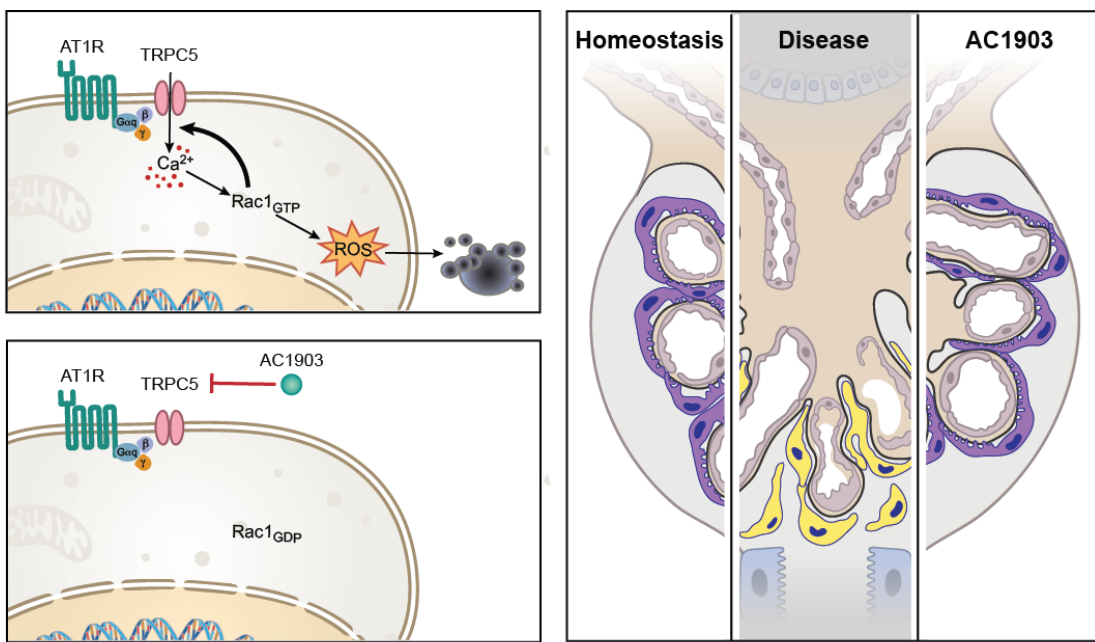


**Fig. S10. Treatment with AC1903 is podocyte-protective.**

Schematic model of the molecular mechanism of AC1903 at the cellular level (left), and the podocyte-protective effect of AC1903 treatment *in vivo* (right). On the left, Rac1 triggers TRPC5 activity as well as the generation of ROS.  $\text{Ca}^{2+}$  influx through TRPC5 perpetuates the injury through further activation of Rac1 (upper). This disease pathway is disrupted by AC1903, which blocks TRPC5 channels, prevents ROS production and protects from podocyte loss (lower). On the right, during homeostasis, healthy podocytes (purple) are attached to the glomerular basement membrane through intact foot processes. In the setting of progressive disease, Rac1-TRPC5 signaling in podocytes (yellow) leads to podocyte loss, likely due to a combination of detachment from the basement membrane and/or cell death. Treatment with AC1903 prevents podocyte loss.

**Table S1. Kinase specificity of AC1903**

Kinase name	Activity to DMSO (%)	Control compound IC <sub>50</sub> (M)	Control compound
ABL1	105.08	5.93E-08	Staurosporine
ABL2/ARG	104.25	1.83E-08	Staurosporine
ACK1	93.71	2.55E-08	Staurosporine
AKT1	97.95	7.03E-09	Staurosporine
AKT2	97.40	2.66E-08	Staurosporine
AKT3	95.06	5.25E-09	Staurosporine
ALK	97.66	1.92E-09	Staurosporine
ALK1/ACVRL1	96.59	2.22E-08	LDN193189
ALK2/ACVR1	100.20	1.68E-08	LDN193189
ALK3/BMPR1A	100.42	3.71E-08	LDN193189
ALK4/ACVR1B	98.03	4.05E-07	LDN193189
ALK5/TGFRB1	101.82	4.23E-07	LDN193189
ALK6/BMPR1B	92.01	8.33E-09	LDN193189
ARAF	90.35	1.73E-08	GW5074
ARK5/NUAK1	103.56	1.34E-09	Staurosporine
ASK1/MAP3K5	95.16	2.95E-08	Staurosporine
Aurora A	102.23	1.41E-09	Staurosporine
Aurora B	92.38	4.63E-09	Staurosporine
Aurora C	95.78	5.52E-09	Staurosporine
AXL	86.30	4.77E-09	Staurosporine
BLK	95.24	1.72E-09	Staurosporine
BMPR2	124.69	7.49E-08	Staurosporine
BMX/ETK	101.14	5.27E-09	Staurosporine
BRAF	104.04	2.56E-08	GW5074
BRK	93.73	2.34E-07	Staurosporine
BRSK1	98.58	5.88E-10	Staurosporine
BRSK2	93.80	1.38E-09	Staurosporine

BTK	100.27	2.38E-08	Staurosporine
c-Kit	95.56	1.30E-07	Staurosporine
c-MER	103.52	1.13E-08	Staurosporine
c-MET	78.27	1.74E-07	Staurosporine
c-Src	94.78	2.60E-09	Staurosporine
CAMK1a	92.21	3.50E-09	Staurosporine
CAMK1b	85.86	6.62E-09	Staurosporine
CAMK1d	97.40	4.20E-10	Staurosporine
CAMK1g	87.57	3.65E-09	Staurosporine
CAMK2a	97.98	5.96E-11	Staurosporine
CAMK2b	95.04	7.56E-11	Staurosporine
CAMK2d	101.41	7.03E-11	Staurosporine
CAMK2g	98.78	3.68E-10	Staurosporine
CAMK4	93.48	1.36E-07	Staurosporine
CAMKK1	93.47	5.81E-08	Staurosporine
CAMKK2	84.62	3.75E-08	Staurosporine
CD7/DBF4	94.20	4.13E-08	Staurosporine
CDK1/cyclin A	95.28	3.69E-09	Staurosporine
CDK1/cyclin B	92.40	2.87E-09	Staurosporine
CDK1/cyclin E	93.97	3.73E-09	Staurosporine
CDK14/cyclin Y (PFTK1)	106.51	2.24E-07	Staurosporine
CDK16/cyclin Y (PCTAIRE)	109.29	2.11E-08	Staurosporine
CDK17/cyclin Y (PCTK2)	83.80	1.61E-08	Staurosporine
CDK18/cyclin Y (PCTK3)	112.13	3.07E-08	Staurosporine
CDK19/cyclin C	96.02	3.54E-11	Staurosporine
CDK2/cyclin A	93.12	8.34E-10	Staurosporine
CDK2/Cyclin A1	101.67	2.00E-09	Staurosporine
CDK2/cyclin E	98.23	3.69E-09	Staurosporine
CDK2/cyclin O	87.29	1.69E-09	Staurosporine
CDK3/cyclin E	97.83	3.70E-09	Staurosporine
CDK4/cyclin D1	105.05	1.89E-08	Staurosporine
CDK4/cyclin D3	101.41	5.15E-08	Staurosporine
CDK5/p25	94.28	2.82E-09	Staurosporine

CDK5/p35	98.91	2.66E-09	Staurosporine
CDK6/cyclin D1	98.69	7.41E-09	Staurosporine
CDK6/cyclin D3	93.72	3.48E-08	Staurosporine
CDK7/cyclin H	94.36	5.80E-08	Staurosporine
CDK9/cyclin K	98.11	7.01E-09	Staurosporine
CDK9/cyclin T1	91.26	6.22E-09	Staurosporine
CDK9/cyclin T2	90.82	4.27E-09	Staurosporine
CHK1	106.10	1.79E-10	Staurosporine
CHK2	100.50	7.20E-09	Staurosporine
CK1a1	91.07	3.39E-06	Staurosporine
CK1a1L	93.80	2.02E-06	Staurosporine
CK1d	98.28	2.12E-07	D4476
CK1epsilon	97.20	3.59E-07	D4476
CK1g1	92.57	9.09E-06	Staurosporine
CK1g2	89.18	1.86E-06	Staurosporine
CK1g3	96.81	2.32E-06	Staurosporine
CK2a	92.88	1.23E-07	GW5074
CK2a2	91.35	8.19E-07	Staurosporine
CLK1	101.60	1.56E-08	Staurosporine
CLK2	100.90	7.31E-09	Staurosporine
CLK3	98.36	2.04E-06	Staurosporine
CLK4	95.60	5.02E-08	Staurosporine
COT1/MAP3K8	87.86	8.42E-06	Ro-31-8220
CSK	98.58	1.82E-08	Staurosporine
CTK/MATK	81.84	6.08E-07	Staurosporine
DAPK1	58.65	9.86E-09	Staurosporine
DAPK2	96.32	7.92E-09	Staurosporine
DCAMKL1	90.28	1.23E-07	Staurosporine
DCAMKL2	95.79	7.83E-08	Staurosporine
DDR1	91.11	2.91E-09	Staurosporine
DDR2	100.40	5.61E-10	Staurosporine
DLK/MAP3K12	91.79	4.29E-07	Staurosporine
DMPK	99.97	3.14E-08	Staurosporine

DMPK2	98.94	5.25E-10	Staurosporine
DRAK1/STK17A	100.05	2.49E-08	Staurosporine
DYRK1/DYRK1A	100.89	3.69E-09	Staurosporine
DYRK1B	93.98	1.15E-09	Staurosporine
DYRK2	100.15	2.22E-07	Staurosporine
DYRK3	104.10	3.47E-08	Staurosporine
DYRK4	102.32	3.04E-06	GW5074
EGFR	101.81	1.09E-07	Staurosporine
EPHA1	102.29	1.36E-07	Staurosporine
EPHA2	99.25	6.95E-08	Staurosporine
EPHA3	90.58	2.43E-08	Staurosporine
EPHA4	97.58	2.47E-08	Staurosporine
EPHA5	111.95	3.13E-08	Staurosporine
EPHA6	94.03	3.68E-08	Staurosporine
EPHA7	96.32	5.19E-08	Staurosporine
EPHA8	98.76	1.33E-07	Staurosporine
EPHB1	99.44	3.53E-08	Staurosporine
EPHB2	102.19	7.99E-08	Staurosporine
EPHB3	100.36	1.34E-06	Staurosporine
EPHB4	95.97	1.92E-07	Staurosporine
ERBB2/HER2	97.42	1.17E-07	Staurosporine
ERBB4/HER4	102.71	2.68E-07	Staurosporine
ERK1	102.47	3.32E-08	SCH772984
ERK2/MAPK1	98.39	2.04E-08	SCH772984
ERK5/MAPK7	104.71	1.36E-05	Staurosporine
ERK7/MAPK15	110.46	1.30E-08	Staurosporine
ERN1/IRE1	83.31	9.58E-08	Staurosporine
ERN2/IRE2	94.64	7.06E-08	Staurosporine
FAK/PTK2	99.15	2.78E-08	Staurosporine
FER	103.69	3.50E-10	Staurosporine
FES/FPS	92.47	1.55E-09	Staurosporine
FGFR1	89.17	4.11E-09	Staurosporine
FGFR2	96.57	2.63E-09	Staurosporine

FGFR3	77.97	7.60E-09	Staurosporine
FGFR4	88.37	1.05E-07	Staurosporine
FGR	94.88	1.06E-09	Staurosporine
FLT1/VEGFR1	98.40	1.07E-08	Staurosporine
FLT3	102.12	1.89E-09	Staurosporine
FLT4/VEGFR3	104.85	1.68E-09	Staurosporine
FMS	96.39	1.75E-09	Staurosporine
FRK/PTK5	99.78	2.13E-08	Staurosporine
FYN	106.96	2.28E-09	Staurosporine
GCK/MAP4K2	89.56	9.29E-10	Staurosporine
GLK/MAP4K3	99.38	1.14E-10	Staurosporine
GRK1	96.24	3.77E-08	Staurosporine
GRK2	104.01	9.92E-07	Staurosporine
GRK3	98.74	9.45E-07	Staurosporine
GRK4	98.66	1.00E-07	Staurosporine
GRK5	108.29	9.29E-08	Staurosporine
GRK6	102.11	4.91E-08	Staurosporine
GRK7	92.32	5.65E-09	Staurosporine
GSK3a	108.02	6.23E-09	Staurosporine
GSK3b	72.55	4.53E-09	Staurosporine
Haspin	91.97	5.05E-08	Staurosporine
HCK	95.92	2.44E-09	Staurosporine
HGK/MAP4K4	91.71	4.95E-10	Staurosporine
HIPK1	100.26	4.69E-07	Ro-31-8220
HIPK2	107.48	9.86E-07	Staurosporine
HIPK3	106.80	6.47E-07	Staurosporine
HIPK4	100.44	5.00E-07	Staurosporine
HPK1/MAP4K1	99.02	8.33E-08	Ro-31-8220
IGF1R	99.00	5.53E-08	Staurosporine
IKKa/CHUK	81.29	1.00E-07	Staurosporine
IKKb/IKBKB	96.41	3.29E-07	Staurosporine
IKKe/IKBKE	104.54	4.41E-10	Staurosporine
IR	93.02	2.19E-08	Staurosporine

IRAK1	121.56	9.22E-08	Staurosporine
IRAK4	104.05	9.96E-09	Staurosporine
IRR/INSRR	96.68	1.15E-08	Staurosporine
ITK	100.61	1.50E-08	Staurosporine
JAK1	100.27	7.87E-10	Staurosporine
JAK2	107.59	2.84E-10	Staurosporine
JAK3	100.77	1.11E-10	Staurosporine
JNK1	101.64	8.30E-07	Staurosporine
JNK2	102.95	1.89E-06	Staurosporine
JNK3	102.02	8.15E-07	JNKi VIII
KDR/VEGFR2	97.82	1.41E-08	Staurosporine
KHS/MAP4K5	93.13	2.48E-10	Staurosporine
KSR1	90.00	4.75E-06	Staurosporine
KSR2	102.37	6.82E-06	Staurosporine
LATS1	98.92	1.81E-08	Staurosporine
LATS2	99.55	9.22E-09	Staurosporine
LCK	93.62	2.48E-09	Staurosporine
LCK2/ICK	112.74	1.29E-07	Staurosporine
LIMK1	94.95	1.35E-09	Staurosporine
LIMK2	102.80	9.52E-08	Staurosporine
LKB1	103.20	4.16E-08	Staurosporine
LOK/STK10	92.59	7.86E-08	Ro-31-8220
LRRK2	101.14	5.73E-09	Staurosporine
LYN	92.26	9.75E-10	Staurosporine
LYN B	105.94	4.66E-09	Staurosporine
MAK	95.35	2.45E-08	Staurosporine
MAPKAPK2	99.16	1.41E-07	Staurosporine
MAPKAPK3	101.86	1.88E-06	Staurosporine
MAPKAPK5/PRAK	106.66	4.35E-07	Staurosporine
MARK1	106.00	3.54E-10	Staurosporine
MARK2/PAR-1Ba	101.51	1.66E-10	Staurosporine
MARK3	103.72	5.42E-10	Staurosporine
MARK4	98.50	1.79E-10	Staurosporine

MEK1	99.71	3.18E-08	Staurosporine
MEK2	98.26	6.34E-08	Staurosporine
MEK3	100.28	8.73E-09	Staurosporine
MEK5	101.22	4.47E-08	Staurosporine
MEKK1	99.65	5.68E-07	Staurosporine
MEKK2	84.68	9.47E-08	Staurosporine
MEKK3	129.68	4.63E-08	Staurosporine
MEKK6	92.12	3.87E-07	Staurosporine
MELK	94.66	6.18E-10	Staurosporine
MINK/MINK1	108.27	7.86E-10	Staurosporine
MKK4	95.68	1.76E-06	Staurosporine
MKK6	101.08	4.91E-09	Staurosporine
MKK7	107.88	1.69E-06	Staurosporine
MLCK/MYLK	92.57	1.05E-07	Staurosporine
MLCK2/MYLK2	96.22	1.91E-08	Staurosporine
MLK1/MAP3K9	96.34	1.46E-09	Staurosporine
MLK2/MAP3K10	90.79	2.72E-09	Staurosporine
MLK3/MAP3K11	104.53	4.51E-09	Staurosporine
MLK4	107.09	2.04E-06	Staurosporine
MNK1	98.54	8.01E-08	Staurosporine
MNK2	99.68	2.54E-08	Staurosporine
MRCKa/CDC42BPA	117.02	6.67E-09	Staurosporine
MRCKb/CDC42BPB	104.32	4.87E-09	Staurosporine
MSK1/RPS6KA5	107.36	6.11E-10	Staurosporine
MSK2/RPS6KA4	92.31	4.99E-09	Staurosporine
MSSK1/STK23	88.94	1.87E-06	Staurosporine
MST1/STK4	109.43	1.16E-09	Staurosporine
MST2/STK3	101.27	5.50E-09	Staurosporine
MST3/STK24	72.54	4.12E-09	Staurosporine
MST4	85.87	4.80E-09	Staurosporine
MUSK	97.91	1.56E-07	Staurosporine
MYLK3	101.03	1.69E-07	Staurosporine
MYLK4	101.18	5.93E-08	Staurosporine

MYO3A	100.59	2.94E-08	Staurosporine
MYO3b	98.70	6.87E-09	Staurosporine
NEK1	102.72	1.33E-08	Staurosporine
NEK11	80.53	4.76E-07	Staurosporine
NEK2	95.73	1.25E-06	Staurosporine
NEK3	96.83	9.47E-05	Staurosporine
NEK4	94.47	1.92E-07	Staurosporine
NEK5	90.10	5.29E-08	Staurosporine
NEK6	101.82	1.67E-05	PKR Inhibitor
NEK7	89.96	5.04E-06	PKR Inhibitor
NEK8	91.59	4.30E-08	Staurosporine
NEK9	98.90	2.02E-07	Staurosporine
NIM1	99.36	1.54E-07	Staurosporine
NLK	106.15	1.68E-07	Staurosporine
OSR1/OXSR1	96.71	1.08E-07	Staurosporine
P38a/MAPK14	102.65	1.55E-08	SB202190
P38b/MAPK11	101.01	3.03E-08	SB202190
P38d/MAPK13	104.57	1.56E-07	Staurosporine
P38g	109.30	2.03E-07	Staurosporine
p70S6K/RPS6KB1	97.87	5.05E-10	Staurosporine
p70S6Kb/RPS6KB2	100.12	1.48E-09	Staurosporine
PAK1	98.48	4.33E-10	Staurosporine
PAK2	98.62	2.78E-09	Staurosporine
PAK3	75.53	7.31E-10	Staurosporine
PAK4	113.00	4.12E-08	Staurosporine
PAK5	105.70	7.40E-09	Staurosporine
PAK6	107.25	2.97E-08	Staurosporine
PASK	94.37	1.13E-08	Staurosporine
PBK/TOPK	105.70	1.44E-07	Staurosporine
PDGFRa	96.52	7.03E-10	Staurosporine
PDGFRb	90.40	3.29E-09	Staurosporine
PDK1/PDPK1	107.28	5.45E-10	Staurosporine
PEAK1	103.83	2.39E-09	Staurosporine

PHKg1	89.70	2.25E-09	Staurosporine
PHKg2	103.79	6.75E-10	Staurosporine
PIM1	94.63	4.44E-09	Staurosporine
PIM2	105.21	5.13E-08	Staurosporine
PIM3	117.70	1.52E-10	Staurosporine
PKA	106.33	1.48E-09	Staurosporine
PKAcb	97.23	1.14E-09	Staurosporine
PKAcg	98.28	3.18E-09	Staurosporine
PKCa	104.07	6.25E-10	Staurosporine
PKCb1	95.61	5.32E-09	Staurosporine
PKCb2	109.65	2.18E-09	Staurosporine
PKCd	107.67	2.16E-10	Staurosporine
PKCepsilon	95.89	1.94E-10	Staurosporine
PKCeta	89.30	6.52E-10	Staurosporine
PKCg	96.90	2.49E-09	Staurosporine
PKCiota	100.29	1.68E-08	Staurosporine
PKCmu/PRKD1	101.01	1.89E-09	Staurosporine
PKCnu/PRKD3	93.73	9.81E-10	Staurosporine
PKCtheta	103.37	2.23E-09	Staurosporine
PKCzeta	100.47	7.69E-08	Staurosporine
PKD2/PRKD2	94.62	1.20E-09	Staurosporine
PKG1a	94.98	1.30E-09	Staurosporine
PKG1b	96.73	2.64E-09	Staurosporine
PKG2/PRKG2	98.66	1.38E-09	Staurosporine
PKN1/PRK1	96.96	5.45E-11	Staurosporine
PKN2/PRK2	91.58	2.58E-09	Staurosporine
PKN3/PRK3	100.12	1.39E-08	Staurosporine
PLK1	98.70	2.06E-07	Staurosporine
PLK2	101.31	3.59E-07	Staurosporine
PLK3	99.91	3.59E-09	BI2536
PLK4/SAK	91.73	1.01E-08	Staurosporine
PRKX	104.56	2.11E-09	Staurosporine
PYK2	97.30	9.79E-09	Staurosporine

RAF1	97.03	1.02E-08	GW5074
RET	95.63	2.81E-09	Staurosporine
RIPK2	104.94	1.40E-07	Staurosporine
RIPK3	95.05	1.40E-06	GW5074
RIPK4	103.03	7.22E-07	Staurosporine
RIPK5	95.91	5.02E-08	Staurosporine
ROCK1	97.24	9.30E-10	Staurosporine
ROCK2	103.62	4.58E-10	Staurosporine
RON/MST1R	104.38	2.38E-07	Staurosporine
ROS/ROS1	104.02	1.85E-10	Staurosporine
RSK1	106.74	1.71E-10	Staurosporine
RSK2	94.45	1.22E-10	Staurosporine
RSK3	101.22	3.51E-10	Staurosporine
RSK4	101.69	5.71E-11	Staurosporine
SBK1	98.61	7.79E-08	Staurosporine
SGK1	101.09	1.08E-08	Staurosporine
SGK2	101.28	1.95E-08	Staurosporine
SGK3/SGKL	107.10	1.45E-07	Staurosporine
SIK1	98.18	3.86E-10	Staurosporine
SIK2	107.05	4.32E-10	Staurosporine
SIK3	100.12	9.71E-10	Staurosporine
SLK/STK2	89.48	2.32E-08	Staurosporine
SNARK/NUAK2	94.92	1.85E-09	Staurosporine
SNRK	92.48	1.63E-08	Staurosporine
SRMS	91.38	5.24E-06	Staurosporine
SRPK1	119.91	4.01E-08	Staurosporine
SRPK2	94.21	1.93E-07	Staurosporine
SSTK/TSSK6	92.18	2.00E-07	Staurosporine
STK16	105.22	2.65E-07	Staurosporine
STK21/CIT	89.75	9.77E-07	Staurosporine
STK22D/TSSK1	97.45	6.74E-11	Staurosporine
STK25/YSK1	104.14	3.36E-09	Staurosporine
STK32B/YANK2	110.73	3.89E-08	Staurosporine

STK32C/YANK3	90.07	2.18E-07	Staurosporine
STK33	93.86	2.73E-08	Staurosporine
STK38/NDR1	90.02	9.60E-10	Staurosporine
STK38L/NDR2	102.66	1.50E-09	Staurosporine
STK39/STLK3	96.95	1.08E-08	Staurosporine
SYK	94.76	3.36E-10	Staurosporine
TAK1	97.24	5.02E-08	Staurosporine
TAOK1	101.27	1.84E-09	Staurosporine
TAOK2/TAO1	97.72	6.61E-09	Staurosporine
TAOK3/JIK	100.01	1.66E-09	Staurosporine
TBK1	97.49	2.01E-09	Staurosporine
TEC	98.70	7.12E-08	Staurosporine
TESK1	127.83	4.45E-07	Staurosporine
TESK2	100.23	1.23E-05	Staurosporine
TGFBR2	99.44	1.10E-07	LDN193189
TIE2/TEK	97.41	8.45E-08	Staurosporine
TLK1	104.30	4.86E-08	Staurosporine
TLK2	107.51	3.43E-09	Staurosporine
TNIK	89.57	2.91E-10	Staurosporine
TNK1	98.97	4.43E-09	Staurosporine
TRKA	91.84	4.03E-09	Staurosporine
TRKB	86.73	1.95E-10	Staurosporine
TRKC	96.48	2.53E-10	Staurosporine
TSSK2	96.04	6.58E-09	Staurosporine
TSSK3/STK22C	98.46	1.18E-08	Staurosporine
TTBK1	95.78	1.48E-05	SB202190
TTBK2	90.82	3.09E-06	SB202190
TXK	94.75	2.56E-08	Staurosporine
TYK1/LTK	103.11	1.86E-08	Staurosporine
TYK2	110.54	2.93E-10	Staurosporine
TYRO3/SKY	101.74	2.21E-09	Staurosporine
ULK1	99.46	1.28E-08	Staurosporine
ULK2	97.62	7.89E-09	Staurosporine

ULK3	99.08	4.51E-09	Staurosporine
VRK1	91.39	8.20E-07	Ro-31-8220
VRK2	98.92	1.96E-05	Ro-31-8220
WEE1	99.50	6.91E-08	Wee-1 Inhibitor
WNK1	89.37	2.31E-05	Staurosporine
WNK2	99.42	1.93E-06	Staurosporine
WNK3	94.67	2.28E-06	Wee-1 Inhibitor
YES/YES1	100.48	2.09E-09	Staurosporine
YSK4/MAP3K19	92.16	2.51E-08	Staurosporine
ZAK/MLTK	97.10	1.51E-06	GW5074
ZAP70	103.03	1.77E-08	Staurosporine
ZIPK/DAPK3	90.23	4.07E-09	Staurosporine

**Table S2. Differentially expressed genes**

AT1R Tg Veh vs. WT Veh		
Gene Name	Log2 Fold Change	Adjusted p-value
SGCG	13.2822	2.01E-16
NWD2	8.4219	1.07E-04
TMEM114	7.9357	1.72E-03
EPX	5.7275	2.94E-18
DRP2	4.9079	3.97E-02
KCNA6	4.8644	4.84E-03
GDF5	3.6951	2.59E-14
RUNX2	3.6171	1.58E-26
SOST	3.6014	2.13E-06
SYNPR	3.4125	3.06E-13
TGFB3	3.3927	3.29E-30
GSTA4	2.9880	3.51E-02
LYPD1	2.9408	2.01E-16
QRFPR	2.8130	8.92E-03
TMEM178B	2.8047	3.61E-03
SLC25A48	2.7959	1.23E-02

GLP1R	2.7799	7.55E-08
ADRA1A	2.7616	6.66E-03
IGSF10	2.7409	3.25E-12
ADRA2B	2.6653	1.24E-06
SLC10A5	2.6598	3.69E-02
NDUFB4	2.5844	2.82E-02
MAP3K15	2.5721	3.36E-02
BLOC1S3	2.5663	3.51E-02
SPINK1	2.4583	1.63E-02
PBX4	2.4291	1.08E-02
COL1A1	2.4093	2.03E-07
ADAMTS18	2.3441	5.99E-04
B4GALNT2	2.2858	3.87E-02
LRRC19	2.2508	1.91E-03
PROZ	2.1722	2.23E-04
NRG1	2.1690	2.22E-02
MAPK4	2.1570	1.03E-02
SLC28A1	2.0724	2.04E-02
PDGFC	2.0571	3.41E-02
KIAA1244	2.0346	4.26E-03
FAM46C	2.0188	2.17E-02
ENPP6	1.9717	3.01E-02
MAOB	1.9252	6.33E-04
TRPV1	1.9229	2.24E-04
KIAA1919	1.9123	1.75E-02
ACMSD	1.8979	1.05E-03
FBP1	1.8861	6.33E-04
RAVER2	1.8821	1.02E-02
RRAGD	1.8787	2.66E-02
FAM83G	1.8659	1.84E-03
MAP7	1.8583	8.93E-04
APCS	1.8516	1.61E-03
FGA	1.8499	3.57E-02

RBM47	1.8491	2.13E-02
STRA6	1.8448	2.64E-02
COL6A6	1.8390	2.32E-02
SULT1C2	1.8253	5.52E-03
FGF1	1.8138	1.03E-02
HYKK	1.8099	1.76E-02
SSTR3	1.8053	1.10E-02
SLC44A3	1.8038	3.27E-02
SULT1C2	1.7958	2.22E-03
AASS	1.7843	2.84E-04
DNAH7	1.7836	8.99E-03
GRAMD1B	1.7820	5.02E-04
CLCN5	1.7819	2.92E-02
COL4A6	1.7777	5.99E-04
GSTA5	1.7770	1.40E-03
GBA3	1.7735	4.58E-03
SLC5A12	1.7713	1.26E-03
EFHC2	1.7484	3.77E-03
ALPL	1.7371	2.13E-19
ALDH8A1	1.7297	4.67E-03
PCSK1N	1.7225	3.01E-02
KL	1.7213	1.20E-02
SULT1C2	1.7179	2.64E-02
HNF4A	1.7153	5.86E-03
IGSF11	1.7053	7.03E-03
KCNMB4	1.7045	2.92E-02
CES2	1.7002	2.22E-03
C4A	1.6994	5.35E-03
SLC15A1	1.6946	7.18E-03
NOX4	1.6921	2.65E-03
DDC	1.6873	6.28E-03
PSAT1	1.6871	1.81E-02
PVRL1	1.6814	2.35E-02

KIF11	1.6810	2.65E-03
MOB3B	1.6782	1.99E-02
PHGDH	1.6773	3.06E-03
TMEM174	1.6673	1.23E-02
GCAT	1.6666	1.44E-02
CIDEB	1.6621	1.30E-02
C7orf57	1.6569	2.40E-02
SORCS2	1.6567	2.39E-03
TSTD1	1.6519	8.99E-03
KIAA1919	1.6484	4.34E-03
SLC26A1	1.6482	4.01E-03
SLC13A1	1.6466	2.73E-04
ABAT	1.6445	1.05E-03
LAMA1	1.6430	2.22E-03
ASS1	1.6391	1.92E-03
SLC2A2	1.6294	1.31E-02
SLC16A14	1.6242	1.51E-02
GLDC	1.6228	4.61E-02
EPS8	1.6215	5.89E-03
SLC16A12	1.6185	7.46E-03
ROS1	1.6099	4.67E-03
RAB3IL1	1.6043	2.40E-02
MGAT3	1.6033	1.41E-02
SLC1A1	1.6008	4.64E-03
ERBB3	1.6001	1.08E-02
DNAJC6	1.5949	2.39E-02
TCEA3	1.5876	1.50E-02
CA12	1.5855	1.92E-03
AKR1C2	1.5780	5.87E-05
TPH1	1.5758	1.68E-04
GOLT1A	1.5733	3.46E-02
SPTA1	1.5733	3.27E-02
CUBN	1.5728	5.59E-03

HAO2	1.5720	1.92E-03
CES2	1.5694	1.19E-02
ALDOB	1.5632	8.56E-04
OLFML1	1.5599	1.47E-03
GLYCTK	1.5591	1.90E-03
PAH	1.5569	1.64E-03
AK4	1.5545	5.12E-03
FERMT1	1.5518	4.11E-02
CSF2RB	1.5499	7.83E-03
SHMT1	1.5467	1.82E-02
WDR72	1.5464	2.71E-02
SLC16A4	1.5409	1.40E-03
CDKL1	1.5384	7.12E-06
METTL7B	1.5339	3.75E-02
XPNPEP2	1.5320	3.04E-03
C4orf19	1.5293	1.26E-03
SLC22A23	1.5289	1.26E-02
AKR1C4	1.5281	4.75E-03
SLC7A9	1.5279	1.75E-02
SLC7A8	1.5219	7.83E-03
CMBL	1.5150	1.83E-05
SLC43A2	1.5143	1.47E-03
ICOSLG	1.5140	3.80E-02
PRR15	1.5113	1.83E-02
MGAM	1.5084	2.34E-02
SGK2	1.5076	4.08E-02
ADH1C	1.5061	2.53E-02
TTC36	1.5011	2.38E-04
DPYS	1.4992	2.43E-02
DUSP15	1.4990	7.18E-03
PRSS12	1.4985	2.99E-02
PDZK1	1.4976	4.75E-03
HNF1B	1.4970	3.80E-03

SEMA5B	1.4958	1.60E-04
MYRF	1.4949	1.05E-03
DECR2	1.4890	1.09E-03
ABCG2	1.4869	6.90E-03
SLC7A7	1.4816	4.66E-03
PKLR	1.4742	4.64E-03
DDAH1	1.4719	4.84E-03
PTGDS	1.4711	2.34E-02
GLYAT	1.4658	7.33E-05
SORD	1.4644	1.05E-03
PCK1	1.4640	7.83E-03
DDO	1.4612	1.40E-02
IYD	1.4563	1.62E-02
DGKG	1.4519	1.75E-02
ANK3	1.4492	1.23E-02
ESPN	1.4484	3.66E-02
ACSS1	1.4478	5.54E-03
EHHADH	1.4460	2.25E-02
OGDHL	1.4424	4.47E-02
FMO1	1.4379	1.61E-02
USH1C	1.4338	1.99E-02
FAM151A	1.4282	6.60E-03
PTER	1.4211	8.99E-03
GAS2	1.4192	3.45E-02
SULT1C2	1.4190	1.94E-03
ASPA	1.4134	3.06E-03
VIL1	1.4113	3.09E-02
KMO	1.4091	1.19E-02
SLIT2	1.4052	3.67E-02
ABCG2	1.4027	4.91E-05
LGMN	1.3996	4.68E-03
CRYL1	1.3986	1.10E-02
LRP3	1.3950	2.32E-02

ADAMTS15	1.3948	1.89E-02
SMIM24	1.3912	7.24E-03
SLC27A2	1.3894	2.15E-03
MFAP3L	1.3881	3.84E-02
ADAMTS8	1.3871	2.37E-02
SLC22A1	1.3845	4.18E-03
MSRA	1.3771	1.12E-02
THY1	1.3753	1.19E-03
ERICH4	1.3750	3.01E-03
SAT2	1.3735	6.48E-03
CA2	1.3735	3.19E-03
SLC22A8	1.3700	1.30E-02
IDH1	1.3697	4.87E-03
EPB41L3	1.3676	1.15E-02
SULT1C2	1.3614	2.09E-02
DAO	1.3607	7.85E-03
BDH2	1.3593	2.22E-02
GLIS3	1.3574	3.76E-02
SLC5A2	1.3559	3.77E-03
CHCHD10	1.3501	1.11E-03
TMEM144	1.3485	3.69E-02
SLC22A9	1.3454	4.52E-02
SPINK1	1.3453	4.16E-06
SLC9A3	1.3441	3.78E-02
NEURL2	1.3426	2.67E-02
TMEM27	1.3408	2.01E-03
ACSS3	1.3407	2.28E-02
ALDH1L1	1.3406	1.75E-02
CCDC37	1.3399	1.06E-03
CES1	1.3372	1.10E-02
SLC25A13	1.3364	2.32E-02
ACOT4	1.3353	4.81E-02
PKP3	1.3330	2.71E-02

CLYBL	1.3320	6.75E-03
UBE3D	1.3280	4.52E-02
SLC16A10	1.3263	4.82E-02
HRSP12	1.3252	3.06E-03
GALM	1.3222	6.71E-04
ASPDH	1.3218	9.03E-03
ALDH7A1	1.3217	1.30E-02
ANPEP	1.3170	2.13E-02
SLC13A2	1.3164	3.41E-02
ACSM2A	1.3139	7.22E-03
SLC34A3	1.3131	2.36E-03
MAN1A1	1.3128	2.65E-03
SERPINC1	1.3124	2.39E-02
PLS1	1.3117	2.74E-02
TPMT	1.3093	3.04E-03
ATP6V0A4	1.3074	8.52E-03
CYP4A22	1.3074	1.76E-02
AGXT2	1.3064	3.04E-03
GRAMD4	1.3051	2.71E-02
DCXR	1.3041	3.06E-03
GATM	1.3035	1.05E-02
UPB1	1.3031	5.62E-03
CYP4A11	1.3024	4.06E-02
C15orf59	1.3020	2.74E-02
SLC13A3	1.3011	7.18E-03
SPP2	1.2962	1.81E-02
PC	1.2944	4.58E-03
L3HYPDH	1.2901	4.61E-03
FAM213B	1.2846	4.01E-03
HNF1A	1.2843	2.80E-02
CYP4F11	1.2834	1.10E-02
AMN	1.2792	2.67E-02
MAB21L3	1.2779	7.64E-03

NAPSA	1.2770	2.31E-02
PIGR	1.2749	4.24E-02
DHTKD1	1.2743	7.14E-03
SLC34A1	1.2730	4.43E-03
ABCC2	1.2720	2.19E-02
NKD2	1.2698	2.35E-03
BHMT2	1.2696	4.58E-03
FN3K	1.2695	1.81E-02
CTH	1.2689	1.47E-02
PERP	1.2637	2.32E-02
ADPRHL1	1.2622	3.09E-02
CBS	1.2593	2.40E-02
NR1H4	1.2536	1.33E-02
WWC1	1.2508	2.06E-03
RBP1	1.2474	1.13E-02
HPD	1.2455	4.58E-03
SNX30	1.2445	2.93E-02
SLC25A10	1.2429	1.06E-03
ANKS4B	1.2424	2.51E-02
SCAND1	1.2424	1.62E-02
SLC12A8	1.2392	2.68E-02
CRYZ	1.2385	4.61E-03
SLC5A11	1.2384	9.05E-03
PDZK1IP1	1.2298	6.71E-04
MT1X	1.2294	1.43E-02
SLC38A7	1.2252	4.53E-02
SFXN1	1.2246	4.44E-03
MEP1A	1.2209	3.56E-02
RBPMS2	1.2197	1.27E-03
DNAJC22	1.2152	3.41E-02
CTSH	1.2134	4.82E-05
PLLP	1.2105	4.58E-03
DPP7	1.2080	2.06E-03

SEPHS2	1.2071	6.46E-04
SLC6A13	1.2048	1.16E-02
CLDN2	1.2014	4.62E-05
GSTA4	1.2009	1.44E-03
CELA1	1.1891	3.01E-02
GK	1.1854	8.98E-03
DAPK2	1.1848	3.75E-02
ABCC4	1.1830	4.14E-02
CCBL1	1.1802	3.57E-03
SLC22A6	1.1777	7.50E-04
HPN	1.1771	1.89E-02
CAT	1.1771	1.03E-02
ADHFE1	1.1771	2.55E-02
PROSC	1.1758	2.56E-02
METRN	1.1706	4.91E-05
GSTA3	1.1704	1.15E-03
FZD1	1.1666	1.78E-02
SUOX	1.1666	9.25E-03
SCLY	1.1662	4.75E-03
GRHPR	1.1662	1.32E-05
ABHD17C	1.1644	2.06E-03
ERRFI1	1.1620	2.59E-03
RNF128	1.1605	2.68E-02
XYLB	1.1594	4.58E-03
PDP2	1.1536	6.69E-03
HAAO	1.1526	1.41E-02
APOM	1.1479	2.63E-02
FAH	1.1452	2.34E-03
H2AFJ	1.1425	7.30E-04
EPCAM	1.1419	1.20E-02
ETV1	1.1408	6.66E-03
CTSC	1.1404	1.84E-02
GLB1L2	1.1401	1.75E-02

NAPRT	1.1396	9.25E-03
TM7SF2	1.1382	4.05E-02
SLC3A1	1.1378	6.85E-03
ALDH6A1	1.1376	7.06E-03
PGPEP1	1.1366	1.28E-02
NAT8	1.1330	4.59E-02
TPM3	1.1328	6.48E-03
PAQR5	1.1314	1.28E-02
DMGDH	1.1276	4.10E-02
CYP2E1	1.1194	2.29E-02
G0S2	1.1190	8.63E-03
PRSS8	1.1187	3.19E-03
SLC22A5	1.1186	4.06E-02
PAK2	1.1176	3.41E-02
ALDH2	1.1149	4.87E-03
SLC29A3	1.1148	1.50E-02
ICAM5	1.1125	2.55E-02
SEZ6L2	1.1111	3.94E-02
C11orf54	1.1100	1.12E-02
SMIM22	1.1087	2.15E-02
GLUL	1.1079	1.76E-02
COBLL1	1.1073	1.15E-02
SLC25A23	1.1062	1.01E-02
ETHE1	1.1016	1.84E-02
GCSH	1.0996	4.43E-03
OXCT1	1.0983	7.22E-03
PECR	1.0979	2.27E-02
ACY1	1.0967	1.38E-02
CELSR2	1.0952	1.30E-02
HGD	1.0950	7.22E-03
TAS1R2	1.0946	6.95E-03
HOGA1	1.0945	2.45E-02
CALML4	1.0925	2.29E-02

OPLAH	1.0918	1.14E-03
GSTZ1	1.0883	8.56E-04
GPD1	1.0830	4.79E-04
TMEM79	1.0790	2.10E-02
PYROXD2	1.0752	5.36E-03
COMT	1.0746	6.36E-03
AKR1E2	1.0746	1.61E-02
PROC	1.0703	4.42E-02
DBI	1.0671	9.27E-05
TSKU	1.0669	9.18E-03
TMPRSS13	1.0655	1.76E-02
STEAP2	1.0643	2.66E-02
AKR7A2	1.0632	1.16E-02
GGH	1.0624	6.02E-05
ACSF2	1.0591	4.27E-02
PEPD	1.0584	9.07E-03
SLC17A3	1.0581	1.23E-02
NDRG1	1.0571	1.76E-02
GNPDA1	1.0503	1.30E-02
DAK	1.0482	2.53E-02
C14orf159	1.0465	4.59E-02
ECI2	1.0462	2.65E-03
LACTB2	1.0420	2.66E-02
PEX11A	1.0411	2.69E-02
CPPED1	1.0353	2.38E-02
SLC6A8	1.0313	6.75E-03
PINK1	1.0299	1.89E-02
GLOD5	1.0289	4.97E-02
AFMID	1.0263	6.85E-03
PDK2	1.0255	9.06E-03
TPRN	1.0252	1.72E-02
FAM20C	1.0211	5.43E-03
LAMB1	1.0191	1.12E-03

CYCS	1.0178	5.27E-03
UGT2B28	1.0177	1.75E-02
RMDN1	1.0172	4.13E-02
MIOX	1.0155	4.58E-03
TFCP2L1	1.0140	2.66E-02
DHRS4L2	1.0109	1.07E-03
FAM195A	1.0095	1.74E-02
PSPH	1.0044	3.10E-02
NABP1	1.0029	2.43E-02
FADS1	1.0028	2.40E-05
RAB11FIP3	1.0017	1.24E-02
SEMA4A	0.9989	2.56E-02
HES6	0.9978	1.04E-02
NDUFC1	0.9976	6.38E-03
GCDH	0.9929	1.04E-02
BCL7A	0.9886	4.47E-02
NQO2	0.9800	2.64E-02
TRPV4	0.9781	1.84E-02
GPRC5C	0.9774	1.09E-03
PBLD	0.9761	1.13E-02
IPP	0.9757	1.35E-02
KCNK5	0.9752	1.09E-02
MRPS34	0.9736	5.35E-03
CDHR5	0.9732	4.18E-02
GPR56	0.9712	5.43E-03
THNSL2	0.9688	2.30E-02
HOOK1	0.9677	4.11E-02
SUSD2	0.9648	2.74E-02
TST	0.9639	2.43E-02
C1orf122	0.9631	4.52E-02
MDH1	0.9586	1.84E-02
GPX1	0.9554	5.24E-03
DDX19A	0.9537	2.59E-04

INMT	0.9519	2.41E-02
CAMK2N1	0.9437	2.28E-02
ITGA6	0.9399	3.69E-02
ATP6V1B2	0.9391	1.60E-02
PLEKHG3	0.9370	7.18E-03
SLC37A4	0.9357	1.39E-02
LACTB	0.9354	1.64E-03
DDR1	0.9302	3.19E-03
PRODH2	0.9289	8.92E-03
VILL	0.9276	2.98E-02
AOC3	0.9274	6.66E-03
FABP3	0.9234	1.13E-02
HS6ST1	0.9218	4.56E-04
SERHL2	0.9205	2.99E-02
KIF12	0.9204	1.47E-02
KHK	0.9140	7.22E-03
PANK1	0.9096	4.26E-02
FAM134B	0.9087	2.17E-02
LDHD	0.9077	3.70E-02
TSPAN33	0.9061	2.30E-02
PDE12	0.8980	3.45E-02
AGAP10	0.8925	1.50E-02
GLB1	0.8886	1.60E-02
SLC9A3R1	0.8826	1.97E-02
CTSB	0.8760	3.65E-02
MPST	0.8726	2.67E-02
UGT1A1	0.8683	6.72E-03
GALNT11	0.8657	2.17E-02
SHMT2	0.8634	3.43E-02
IGF2R	0.8614	2.21E-02
TXNDC17	0.8523	2.42E-02
SUCLG1	0.8519	2.23E-02
PHYHD1	0.8514	3.51E-02

MPC2	0.8483	1.78E-03
FDX1	0.8409	1.77E-02
HSPE1	0.8333	1.82E-03
COX5A	0.8327	1.43E-02
ABHD14B	0.8314	2.64E-02
FMO3	0.8310	1.16E-02
PAX8	0.8277	2.64E-02
FHOD3	0.8264	1.65E-02
ACP5	0.8247	3.81E-02
KLHL25	0.8153	1.48E-02
SLC31A1	0.8111	3.84E-02
ASRGL1	0.8102	2.74E-02
IAH1	0.8095	4.27E-02
ATP5F1	0.8088	2.56E-02
TRAF4	0.7902	2.67E-02
HADH	0.7702	4.08E-02
KRT8	0.7680	1.65E-02
SNTA1	0.7669	3.26E-02
CDH16	0.7541	2.73E-02
SCNM1	0.7527	4.71E-02
ATP5F1	0.7524	1.05E-02
CPQ	0.7484	9.91E-03
ATP1B1	0.7425	4.71E-02
ENO1	0.7399	4.74E-02
HIBADH	0.7399	2.76E-02
MPC1	0.7395	1.17E-02
HSPD1	0.7382	3.62E-02
GLRX5	0.7369	4.13E-02
ATP5G3	0.7348	1.38E-02
UQCRC2	0.7190	4.57E-02
GAPDH	0.7162	2.48E-02
IMMT	0.7159	1.65E-02
COX8A	0.7109	1.76E-02

C8orf82	0.7090	1.89E-02
CISD1	0.7077	8.92E-03
TGM2	0.7058	2.39E-02
ATP5O	0.7024	4.50E-02
GAPDH	0.6957	3.41E-02
ATP5I	0.6694	1.95E-02
VWA5A	0.6538	3.32E-02
CYC1	0.6514	4.32E-02
TPI1	0.6345	1.65E-02
PGAM4	0.6115	4.92E-02
ATP5D	0.6059	1.97E-02
CYBA	0.5814	2.44E-02
NDUFB2	0.5736	2.67E-02
NDUFA4	0.5634	1.58E-02
SOD1	0.5567	4.59E-02
ATP6V0D1	0.5046	4.99E-02
SLC44A2	-0.5068	2.98E-02
PBX2	-0.5147	4.61E-02
NPR1	-0.5353	2.82E-02
CYB5R3	-0.6082	1.17E-02
FAM117B	-0.6115	2.98E-02
TMBIM1	-0.6328	3.77E-02
NOD1	-0.6467	4.11E-02
SERINC5	-0.6566	2.44E-02
TUBA1A	-0.6577	2.67E-02
HPSE	-0.6630	1.74E-02
EMP2	-0.6658	7.91E-03
BCAM	-0.7020	1.65E-02
ABCD4	-0.7076	1.33E-02
KANK1	-0.7288	6.06E-03
TDRP	-0.7296	1.13E-02
PLAT	-0.7414	2.17E-02
FAM65A	-0.7653	7.03E-03

DES	-0.7761	1.47E-02
ANKRD44	-0.7921	3.04E-03
SPON1	-0.8085	2.92E-02
TSPAN8	-0.8457	4.84E-03
TMEM109	-0.8584	8.42E-04
APOL2	-0.9315	1.76E-02
PLTP	-1.0668	2.50E-04
PALD1	-1.1085	7.18E-03
PDE1B	-1.1625	9.27E-05
PDPN	-1.1667	5.13E-04
RHBDL3	-1.1776	2.42E-05
RTP4	-1.1977	4.20E-02
TGIF2	-1.2285	2.93E-02
C10orf10	-1.2426	2.45E-02
CPNE7	-1.2566	1.47E-03
TNNC1	-1.2621	7.86E-04
DCLRE1C	-1.2880	9.37E-04
C1orf159	-1.4474	2.14E-02
ARPP21	-1.4520	4.84E-03
TMEM215	-1.6086	2.43E-04
PLXDC1	-2.2291	1.72E-02
KIF22	-2.2418	3.78E-03
SPEG	-2.3727	7.00E-12
LMOD2	-2.5385	1.24E-03
TBRG1	-2.5951	1.75E-02
C12orf56	-3.1697	2.64E-02
RASSF4	-3.2089	4.92E-02
GSG1	-3.3431	3.29E-17
RSPO1	-3.4963	5.00E-08
UPK3A	-4.6783	4.64E-03

**AT1R Tg AC1903 vs. AT1R Tg Veh**

<b>Gene Name</b>	<b>Log2 Fold Change</b>	<b>Adjusted p-value</b>
ACER2	1.2765	3.00E-03
APOL3	1.2450	4.52E-03
ARHGAP30	2.3284	3.87E-03
B2M	0.8615	9.65E-03
C15orf48	3.3361	7.32E-04
C16orf54	2.5504	3.14E-02
CD4	1.8715	1.41E-02
CORO1A	1.5252	3.66E-02
CYBB	1.7153	1.65E-02
CYP26B1	1.4031	1.54E-03
EGF	1.7385	3.44E-03
EMR1	1.7255	7.58E-03
FCGR2B	1.9650	1.11E-02
FCGR3A	1.9210	4.76E-03
FKBP5	1.2570	9.65E-03
GDA	2.0546	1.95E-02
GLIPR1	2.4187	3.00E-03
HECW2	1.3398	7.32E-04
HLA-B	1.9760	1.65E-02
IL1B	3.0031	9.45E-03
ITGA4	2.5273	7.32E-04
ITGAL	2.0196	3.00E-03
ITGB2	2.0707	8.04E-05
KIAA1551	1.1756	9.65E-03
LCP1	1.5898	3.87E-03
LIFR	1.1826	4.76E-03
MAP3K6	2.0325	1.54E-02
MYO1F	1.8955	1.22E-02
MYO1G	3.1221	2.90E-04
NXPE1	1.5548	5.83E-03
OLR1	1.8384	2.88E-02

POU2F2	7.1731	2.46E-02
PSMB8	1.3147	9.47E-03
PTPRC	1.7489	2.19E-04
RAPGEF5	1.3000	1.65E-02
SENP5	8.1884	1.00E-03
SLFN12	0.9536	3.12E-02
SLFN12L	2.4308	1.35E-08
TMEM2	1.3838	4.76E-03
TRIM2	1.7766	4.65E-02
TYROBP	1.7582	1.26E-02
ZNF260	1.8239	2.64E-02

## References and Notes

1. V. Jha, G. Garcia-Garcia, K. Iseki, Z. Li, S. Naicker, B. Plattner, R. Saran, A. Y.-M. Wang, C.-W. Yang, Chronic kidney disease: Global dimension and perspectives. *Lancet* **382**, 260–272 (2013). [doi:10.1016/S0140-6736\(13\)60687-X](https://doi.org/10.1016/S0140-6736(13)60687-X) [Medline](#)
2. J. K. Inrig, R. M. Califf, A. Tasneem, R. K. Vegunta, C. Molina, J. W. Stanifer, K. Chiswell, U. D. Patel, The landscape of clinical trials in nephrology: A systematic review of Clinicaltrials.gov. *Am. J. Kidney Dis.* **63**, 771–780 (2014). [doi:10.1053/j.ajkd.2013.10.043](https://doi.org/10.1053/j.ajkd.2013.10.043) [Medline](#)
3. V. D. D'Agati, F. J. Kaskel, R. J. Falk, Focal segmental glomerulosclerosis. *N. Engl. J. Med.* **365**, 2398–2411 (2011). [doi:10.1056/NEJMra1106556](https://doi.org/10.1056/NEJMra1106556) [Medline](#)
4. A. Greka, P. Mundel, Cell biology and pathology of podocytes. *Annu. Rev. Physiol.* **74**, 299–323 (2012). [doi:10.1146/annurev-physiol-020911-153238](https://doi.org/10.1146/annurev-physiol-020911-153238) [Medline](#)
5. E. J. Brown, M. R. Pollak, M. Barua, Genetic testing for nephrotic syndrome and FSGS in the era of next-generation sequencing. *Kidney Int.* **85**, 1030–1038 (2014). [doi:10.1038/ki.2014.48](https://doi.org/10.1038/ki.2014.48) [Medline](#)
6. S. Akilesh, H. Suleiman, H. Yu, M. C. Stander, P. Lavin, R. Gbadegesin, C. Antignac, M. Pollak, J. B. Kopp, M. P. Winn, A. S. Shaw, Arhgap24 inactivates Rac1 in mouse podocytes, and a mutant form is associated with familial focal segmental glomerulosclerosis. *J. Clin. Invest.* **121**, 4127–4137 (2011). [doi:10.1172/JCI46458](https://doi.org/10.1172/JCI46458) [Medline](#)
7. H. Y. Gee, P. Saisawat, S. Ashraf, T. W. Hurd, V. Vega-Warner, H. Fang, B. B. Beck, O. Gribouval, W. Zhou, K. A. Diaz, S. Natarajan, R. C. Wiggins, S. Lovric, G. Chernin, D. S. Schoeb, B. Ovunc, Y. Frishberg, N. A. Soliman, H. M. Fathy, H. Goebel, J. Hoefele, L. T. Weber, J. W. Innis, C. Faul, Z. Han, J. Washburn, C. Antignac, S. Levy, E. A. Otto, F. Hildebrandt, ARHGDIA mutations cause nephrotic syndrome via defective RHO GTPase signaling. *J. Clin. Invest.* **123**, 3243–3253 (2013). [doi:10.1172/JCI69134](https://doi.org/10.1172/JCI69134) [Medline](#)
8. H. Yu, M. Artomov, S. Brähler, M. C. Stander, G. Shamsan, M. G. Sampson, J. M. White, M. Kretzler, J. H. Miner, S. Jain, C. A. Winkler, R. D. Mitra, J. B. Kopp, M. J. Daly, A. S. Shaw, A role for genetic susceptibility in sporadic focal segmental glomerulosclerosis. *J. Clin. Invest.* **126**, 1603 (2016). [doi:10.1172/JCI87342](https://doi.org/10.1172/JCI87342) [Medline](#)

9. V. J. Bezzerides, I. S. Ramsey, S. Kotecha, A. Greka, D. E. Clapham, Rapid vesicular translocation and insertion of TRP channels. *Nat. Cell Biol.* **6**, 709–720 (2004). [doi:10.1038/ncb1150](https://doi.org/10.1038/ncb1150) [Medline](#)
10. D. Tian, S. M. P. Jacobo, D. Billing, A. Rozkalne, S. D. Gage, T. Anagnostou, H. Pavenstädt, H.-H. Hsu, J. Schlondorff, A. Ramos, A. Greka, Antagonistic regulation of actin dynamics and cell motility by TRPC5 and TRPC6 channels. *Sci. Signal.* **3**, ra77 (2010). [doi:10.1126/scisignal.2001200](https://doi.org/10.1126/scisignal.2001200) [Medline](#)
11. T. Schaldecker, S. Kim, C. Tarabanis, D. Tian, S. Hakroush, P. Castonguay, W. Ahn, H. Wallentin, H. Heid, C. R. Hopkins, C. W. Lindsley, A. Riccio, L. Buvall, A. Weins, A. Greka, Inhibition of the TRPC5 ion channel protects the kidney filter. *J. Clin. Invest.* **123**, 5298–5309 (2013). [doi:10.1172/JCI71165](https://doi.org/10.1172/JCI71165) [Medline](#)
12. N. Wieder, A. Greka, Calcium, TRPC channels, and regulation of the actin cytoskeleton in podocytes: Towards a future of targeted therapies. *Pediatr. Nephrol.* **31**, 1047–1054 (2016). [doi:10.1007/s00467-015-3224-1](https://doi.org/10.1007/s00467-015-3224-1) [Medline](#)
13. S. Hoffmann, D. Podlich, B. Hähnel, W. Kriz, N. Gretz, Angiotensin II type 1 receptor overexpression in podocytes induces glomerulosclerosis in transgenic rats. *J. Am. Soc. Nephrol.* **15**, 1475–1487 (2004). [doi:10.1097/01.ASN.0000127988.42710.A7](https://doi.org/10.1097/01.ASN.0000127988.42710.A7) [Medline](#)
14. H. H. Hsu, S. Hoffmann, N. Endlich, A. Velic, A. Schwab, T. Weide, E. Schlatter, H. Pavenstädt, Mechanisms of angiotensin II signaling on cytoskeleton of podocytes. *J. Mol. Med. (Berl.)* **86**, 1379–1394 (2008). [doi:10.1007/s00109-008-0399-y](https://doi.org/10.1007/s00109-008-0399-y) [Medline](#)
15. J. M. Richter, M. Schaefer, K. Hill, Riluzole activates TRPC5 channels independently of PLC activity. *Br. J. Pharmacol.* **171**, 158–170 (2014). [doi:10.1111/bph.12436](https://doi.org/10.1111/bph.12436) [Medline](#)
16. M. Miller, J. Shi, Y. Zhu, M. Kustov, J. B. Tian, A. Stevens, M. Wu, J. Xu, S. Long, P. Yang, A. V. Zholos, J. M. Salovich, C. D. Weaver, C. R. Hopkins, C. W. Lindsley, O. McManus, M. Li, M. X. Zhu, Identification of ML204, a novel potent antagonist that selectively modulates native TRPC4/C5 ion channels. *J. Biol. Chem.* **286**, 33436–33446 (2011). [doi:10.1074/jbc.M111.274167](https://doi.org/10.1074/jbc.M111.274167) [Medline](#)
17. T. Hofmann, A. G. Obukhov, M. Schaefer, C. Harteneck, T. Gudermann, G. Schultz, Direct activation of human TRPC6 and TRPC3 channels by diacylglycerol. *Nature* **397**, 259–263 (1999). [doi:10.1038/16711](https://doi.org/10.1038/16711) [Medline](#)

18. M. W. Steffes, D. Schmidt, R. McCrery, J. M. Basgen, Glomerular cell number in normal subjects and in type 1 diabetic patients. *Kidney Int.* **59**, 2104–2113 (2001). [doi:10.1046/j.1523-1755.2001.00725.x](https://doi.org/10.1046/j.1523-1755.2001.00725.x) [Medline](#)
19. A. Weins, J. S. Wong, J. M. Basgen, R. Gupta, I. Daehn, L. Casagrande, D. Lessman, M. Schwartzman, K. Meliambro, J. Patrakka, A. Shaw, K. Tryggvason, J. C. He, S. B. Nicholas, P. Mundel, K. N. Campbell, Dendrin ablation prolongs life span by delaying kidney failure. *Am. J. Pathol.* **185**, 2143–2157 (2015). [doi:10.1016/j.ajpath.2015.04.011](https://doi.org/10.1016/j.ajpath.2015.04.011) [Medline](#)
20. W. Kriz, K. V. Lemley, A potential role for mechanical forces in the detachment of podocytes and the progression of CKD. *J. Am. Soc. Nephrol.* **26**, 258–269 (2015). [doi:10.1681/ASN.2014030278](https://doi.org/10.1681/ASN.2014030278) [Medline](#)
21. M. Freichel, S. H. Suh, A. Pfeifer, U. Schweig, C. Trost, P. Weissgerber, M. Biel, S. Philipp, D. Freise, G. Droogmans, F. Hofmann, V. Flockerzi, B. Nilius, Lack of an endothelial store-operated Ca<sup>2+</sup> current impairs agonist-dependent vasorelaxation in TRP4-/- mice. *Nat. Cell Biol.* **3**, 121–127 (2001). [doi:10.1038/35055019](https://doi.org/10.1038/35055019) [Medline](#)
22. J. M. Richter, M. Schaefer, K. Hill, Clemizole hydrochloride is a novel and potent inhibitor of transient receptor potential channel TRPC5. *Mol. Pharmacol.* **86**, 514–521 (2014). [doi:10.1124/mol.114.093229](https://doi.org/10.1124/mol.114.093229) [Medline](#)
23. L. Buvall, H. Wallentin, J. Sieber, S. Andreeva, H. Y. Choi, P. Mundel, A. Greka, Synaptopodin Is a Coincidence Detector of Tyrosine versus Serine/Threonine Phosphorylation for the Modulation of Rho Protein Crosstalk in Podocytes. *J. Am. Soc. Nephrol.* **28**, 837–851 (2017). [doi:10.1681/ASN.2016040414](https://doi.org/10.1681/ASN.2016040414) [Medline](#)
24. R. F. Wu, Y. C. Xu, Z. Ma, F. E. Nwariaku, G. A. Sarosi Jr., L. S. Terada, Subcellular targeting of oxidants during endothelial cell migration. *J. Cell Biol.* **171**, 893–904 (2005). [doi:10.1083/jcb.200507004](https://doi.org/10.1083/jcb.200507004) [Medline](#)
25. K. L. Pierce, R. T. Premont, R. J. Lefkowitz, Signalling: Seven-transmembrane receptors. *Nat. Rev. Mol. Cell Biol.* **3**, 639–650 (2002). [doi:10.1038/nrm908](https://doi.org/10.1038/nrm908) [Medline](#)
26. K. Sharma, S. Ramachandrarao, G. Qiu, H. K. Usui, Y. Zhu, S. R. Dunn, R. Ouedraogo, K. Hough, P. McCue, L. Chan, B. Falkner, B. J. Goldstein, Adiponectin regulates albuminuria and podocyte function in mice. *J. Clin. Invest.* **118**, 1645–1656 (2008). [Medline](#)

27. Y. H. You, T. Quach, R. Saito, J. Pham, K. Sharma, Metabolomics Reveals a Key Role for Fumarate in Mediating the Effects of NADPH Oxidase 4 in Diabetic Kidney Disease. *J. Am. Soc. Nephrol.* **27**, 466–481 (2016). [doi:10.1681/ASN.2015030302](https://doi.org/10.1681/ASN.2015030302) [Medline](#)
28. J. P. Rapp, Dahl salt-susceptible and salt-resistant rats. A review. *Hypertension* **4**, 753–763 (1982). [doi:10.1161/01.HYP.4.6.753](https://doi.org/10.1161/01.HYP.4.6.753) [Medline](#)
29. J. Zicha, Z. Dobešová, M. Vokurková, H. Rauchová, S. Hojná, M. Kadlecová, M. Behuliak, I. Vaněčková, J. Kuneš, Age-dependent salt hypertension in Dahl rats: Fifty years of research. *Physiol. Res.* **61** (Suppl 1), S35–S87 (2012). [Medline](#)
30. M. R. Garrett, H. Dene, J. P. Rapp, Time-course genetic analysis of albuminuria in Dahl salt-sensitive rats on low-salt diet. *J. Am. Soc. Nephrol.* **14**, 1175–1187 (2003). [doi:10.1097/01.ASN.0000060572.13794.58](https://doi.org/10.1097/01.ASN.0000060572.13794.58) [Medline](#)
31. Y. Yamada, K. Tsuboi, T. Hattori, T. Murase, M. Ohtake, M. Furukawa, J. Ueyama, A. Nishiyama, T. Murohara, K. Nagata, Mechanism underlying the efficacy of combination therapy with losartan and hydrochlorothiazide in rats with salt-sensitive hypertension. *Hypertens. Res.* **34**, 809–816 (2011). [doi:10.1038/hr.2011.34](https://doi.org/10.1038/hr.2011.34) [Medline](#)
32. J. Eckel, P. J. Lavin, E. A. Finch, N. Mukerji, J. Burch, R. Gbadegesin, G. Wu, B. Bowling, A. Byrd, G. Hall, M. Sparks, Z. S. Zhang, A. Homstad, L. Barisoni, L. Birbaumer, P. Rosenberg, M. P. Winn, TRPC6 enhances angiotensin II-induced albuminuria. *J. Am. Soc. Nephrol.* **22**, 526–535 (2011). [doi:10.1681/ASN.2010050522](https://doi.org/10.1681/ASN.2010050522) [Medline](#)
33. M. Riehle, A. K. Büscher, B. O. Gohlke, M. Kaßmann, M. Kolatsi-Joannou, J. H. Bräsen, M. Nagel, J. U. Becker, P. Winyard, P. F. Hoyer, R. Preissner, D. Krautwurst, M. Gollasch, S. Weber, C. Harteneck, TRPC6 G757D Loss-of-Function Mutation Associates with FSGS. *J. Am. Soc. Nephrol.* **27**, 2771–2783 (2016). [Medline](#)
34. A. Riccio, Y. Li, J. Moon, K.-S. Kim, K. S. Smith, U. Rudolph, S. Gapon, G. L. Yao, E. Tsvetkov, S. J. Rodig, A. Van't Veer, E. G. Meloni, W. A. Carlezon Jr., V. Y. Bolshakov, D. E. Clapham, Essential role for TRPC5 in amygdala function and fear-related behavior. *Cell* **137**, 761–772 (2009). [doi:10.1016/j.cell.2009.03.039](https://doi.org/10.1016/j.cell.2009.03.039) [Medline](#)

35. S. Tarazona, P. Furió-Tarí, D. Turrà, A. D. Pietro, M. J. Nueda, A. Ferrer, A. Conesa, Data quality aware analysis of differential expression in RNA-seq with NOISeq R/Bioc package. *Nucleic Acids Res.* **43**, e140 (2015). [10.1093/nar/gkv711](https://doi.org/10.1093/nar/gkv711)  
[Medline](#)
36. M. I. Love, W. Huber, S. Anders, Moderated estimation of fold change and dispersion for RNA-seq data with DESeq2. *Genome Biol.* **15**, 550 (2014).  
[doi:10.1186/s13059-014-0550-8](https://doi.org/10.1186/s13059-014-0550-8) [Medline](#)